ISSN: 2349 2937

A Peer Reviewed Research Journal

SPECTRUM: Science and Technology

Volume: 9: December 15, 2022

x^{a+b} $(x^a)^b = x^{a \times b}$

$= x^{a-b}$ $x^0 = 1$

$)^a = x^a \times x^b$

A Publication of Research and Consultancy Cell
St. Anthony's College
Shillong, Meghalaya, India
www.anthonys.ac.in

Spectrum: Science and Technology, Volume 9(1), 2022

ISSN: 2349-2937

Published by:

Research and Consultancy Cell
St. Anthony's College,
Shillong - 793001
Meghalaya, India

ISSN: 2349 2937

SPECTRUM
Science and Technology

An Annual Peer Reviewed Research Journal

Volume 9 | December 15, 2022

A Publication of
Research and Consultancy Cell

St. Anthony's College
Bomfyle Road, Shillong- 793001
Meghalaya, India
www.anthonys.ac.in
Email: spectrum.st@anthonys.ac.in

Spectrum: Science and Technology
Editorial Board

Dr. Sanku Dey
Department of Statistics
St. Anthony's College, Shillong, Meghalaya
Email: sankud66@gmail.com

Dr. Damanbha Lyngdoh
Department of Zoology
St. Anthony's College, Shillong, Meghalaya
Email: damanshillong@gmail.com

Editors:

Dr. Anjan Das
Department of Computer Science
St. Anthony's College, Shillong, Meghalaya
Email: anjand@anthonys.ac.in

Dr. Shantu Saikia
Department of Physics
St. Anthony's College, Shillong, Meghalaya
Email: shantusaikia@anthonys.ac.in

Dr. Probidita Roychoudhury
Department of Computer Science
St. Anthony's College, Shillong, Meghalaya
Email: probidita@anthonys.ac.in

Dr. Pyniarlang L Nongbri
Department of Biotechnology
St. Anthony's College, Shillong, Meghalaya
Email: pyndrop@gmail.com

Dr. Wympher Langstang
Department of Botany
St. Anthony's College, Shillong, Meghalaya
Email: wlangstang@gmail.com

Dr. V Jennifer J Walang
Department of Geology
St. Anthony's College, Shillong, Meghalaya
Email: vjjwallang@gmail.com

Mr. Thyanswer Challam
Department of Biotechnology
St. Anthony's College, Shillong, Meghalaya
Email: thyanchallam@outlook.com

Dr. Saibadaiahun Nongrum
Department of Biochemistry
St. Anthony's College, Shillong, Meghalaya
Email: saibadaiahun@gmail.com

Dr. Baskhemlang Kshiar
Department of Chemistry
St. Anthony's College, Shillong, Meghalaya
Email: bkshiar@anthonys.ac.in

Dr. Wompherdeiki Khyllep
Department of Mathematics
St. Anthony's College, Shillong, Meghalaya
Email: math1990sac@gmail.com

Editors (Technical):

Mr. Bablu L Rajak
Department of Computer Science
St. Anthony's College, Shillong, Meghalaya
Email: brajak@anthonys.ac.in

Mr. Om Prakash Yadav
Department of Computer Science
St. Anthony's College, Shillong, Meghalaya
Email: omprakash@anthonys.ac.in

Spectrum: Science and Technology

Web: www.anthonys.ac.in

Volume 9 |December 15, 2022

CONTENTS

Research article:

A thought experiment based graphical illustration of the various sections of the characteristic curve of the gas-filled detectors

Rangaraj Bhattacharjee[1]* and Ananya Bhattacharjee[2]

[1]State Cancer Institute, Gauhati Medical College, Guwahati-32, Assam, India
[2]Narayana e-Techno School, Guwahati-01, Assam, India

Article info:
https://doi.org/10.54290/spect/2022.v9.1.0001

Received: July 10th, 2022
Revised: October 10th, 2022
Accepted: October 20th, 2022

Corresponding author:
rangarajphysicistgmch@gmail.com

Abstract: The purpose of this study is to establish similarities between two ideas – a hypothetical thought experiment and a known fact. The study relies on the use of various functions to mathematically quantify the different components of the characteristic or voltage response curve and the operation of the gas-filled detectors. A thought experiment was created by taking into account an imagined particle to travel across space in specific ways. Here, a comparison was made between the characteristic curve and the imagined particle's locus.

Keywords: *Gas filled detectors; parabolic function; hyperbolic function; locus; linear function*

1. INTRODUCTION

In the quest to find new and spectacular things, the inventive and creative nature of humans has produced wonders that have proven to be extremely valuable and useful for the welfare of mankind. The human brain is naturally inclined to seek for answers to questions in order to quell its mania and internal conflict [1]. Sometimes in doing so they seek to draw comparison to show something, explain something, or show distinct aspects of the beauty of nature. Also the theory of everything, a hypothetical framework that tends to explains all observed physical occurrences in the universe and asserts that every event and phenomenon in the cosmos is interconnected, is a fascinating theory of modern times [2]. Physicists often try to explain complicated quantum phenomenon with the happenings in the classical world. In physics, analogies are used frequently. It was adopted by many Nobel laureates in physics, physicists from different eras, practicing and aspiring physics instructors, and students [3]. To mention a few, in Sir Bohr's atomic model, electrons are

How to Cite:
Bhattacharjee and Bhattacharjee (2022). A thought experiment based graphical illustration of the various sections of the characteristic curve of the gas-filled detectors. *Spectrum: Science and Technology, v9 (1), 01-09*. https://doi.org/10.54290/spect/2022.v9.1.0001

arranged in energy levels that resemble bookcase shelves [3], the "Plum-Pudding" model of atom developed by Sir J.J.Thomson [4], the planetary model of atom based on the solar system [5], the Nagaoka Saturnian atom model was made up of revolving electron rings [6, 7], the liquid drop model describes the nucleus as an incompressible liquid droplet, with nucleons acting as the equivalent of molecules in a conventional liquid drop with certain analogies [8], in optical model, atomic nuclei behave like cloudy crystal balls when they are struck by a beam of particles, this interaction is analogous to the behaviour of light [9], with the help of the Sir Bohr's atomic model of electron energy levels, the nuclear shell model describes the atoms' nuclei [10], etc. In this study, the characteristic curve of the gas-filled detectors and the locus of a hypothetical particle were compared to provide a new perspective using a thought experiment. Since such an approach has never been employed before, this study may produce an intriguing approach of connecting various ideas.

2. METHODOLOGY

The sole motive of this investigation was to explain the mechanism of operation and mathematical illustration of the several segments of the characteristic curve of gas-filled detectors. This approach was chosen in order to reach the best conclusion possible, which would simplify as well as abstractly describe the phenomenon. To complement the analysis, a thought experiment has been developed.

2.1 Thought Experiment

A hypothetical particle named "Rangana" was created in this thought experiment, which was designed to move across space in any direction. However, in this thought experiment, only a few distinct ways of its movement were considered. The figure 1 below shows the various paths of "Rangana" travelling in space.

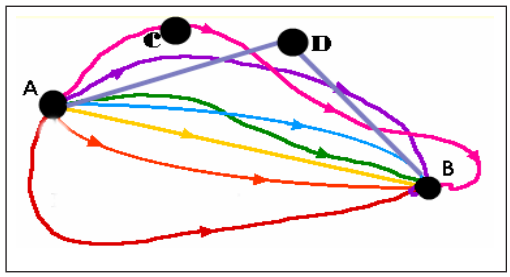

Figure 1. The black dot is the hypothetical particle "Rangana" created in the thought experiment and it can take any path to travel from point A to point B in space.

When the particle is moving from point A to B, point C, D and the straight path from A to B were chosen as shown in Figure 1 from its travel history in order to draw an analogy with the characteristic curve of the gas filled detectors. The analysis was furthered by taking into account the path of the particle "Rangana" in motion under these specific circumstances. In order to explain this, a two-dimensional plane was considered with "X" and "Y" axis to visualize the various paths of the particle "Rangana" as shown in Figure 2 below. The first condition is that the particle is moving from point A to point B under the restriction that its Y- coordinate is constant.

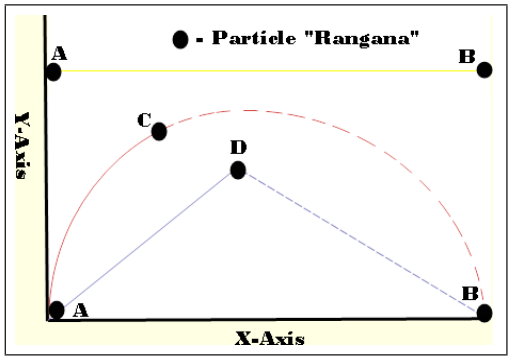

Figure 2. A schematic representation of the various paths of the hypothetical particle "Rangana" created in the thought experiment.

This represents a linear path of the particle. Again, it is considered that the particle is now moving from point A to Point D under the restriction that change in Y coordinate is proportional to the change in X coordinate as shown in the Figure 2 above. This represents a proportional path of the particle. "Rangana" is now moving from point A to point C under the restriction that its distance from a fixed point and from a fixed line is always constant as shown in Figure 2 above. This represents parabolic path.

2.2 Gas Filled Detectors

Human senses are incapable of detecting ionizing radiation. When the energy of the radiation is greater than the gas's ionization potential, it will be able to ionize the gas molecules [11, 12, 13]. The creation of charge pairs in this manner allows for the application of an external electric field to cause them to travel in opposing directions. The outcome is an electric pulse that can be detected by a measurement instrument that is connected to it. The so-called gas filled detectors were built using this method [11,12,13]. There are three different types of Gas-Filled detectors -Ionization Chamber, Proportional Counter, and Geiger Muller Counter - based on the principles of ionization, impact ionization, Townsend avalanche, and chain of avalanche. A characteristic curve explains the function of various gas filled detectors using the applied voltage and pulse amplitude as the variable parameters.

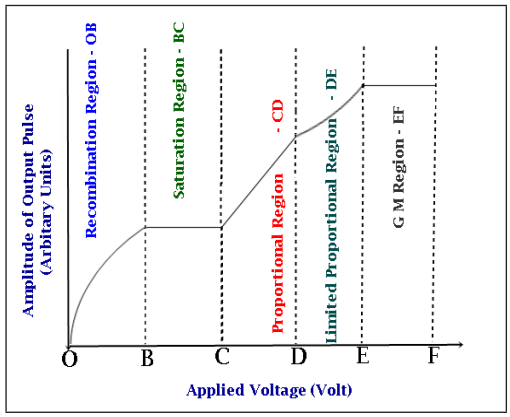

Figure 3. The representation of the various sections of the gas filled detectors – the Characteristic curve.

From the Figure 3 above the following descriptions of the characteristic curve is drawn.

1. Region OB – Recombination region: Ions are created in this region, and because the voltage is so low, they combine again. Charges begin to accumulate and produce counts at higher voltages.

2. Region BC – Saturation region: No

additional charges are available for collection in this area. Thus, there is a plateau.

3. Region CD – Proportional region: Due to the increased voltage that is being delivered in this region, charges are propelled more toward electrodes. Diverging Avalanche is created in this region [11,13]. Gas multiplication increases linearly with applied voltage.

4. Region DE–Limited Proportional region or Nonlinear region: Due to the poor mobility of the positive charges, a space charge barrier of positive charges is generated around the anode [11]. The net electric field is consequently diminished. Because of this, the nature of gas multiplication is non-linear with applied voltage.

5. Region EF – Geiger Muller region: Multiple avalanches are created as a result of the extremely high applied voltage since UV radiation predominates in this region and the condition of criticality is also attained [11,13]. All counts for radiation and energy remain constant since the chain of avalanches stops when it reaches a specific height [11,13]. As a result, the output signal's amplitude never changes.

2.3 Mathematical Representation

Region OB- Recombination region:

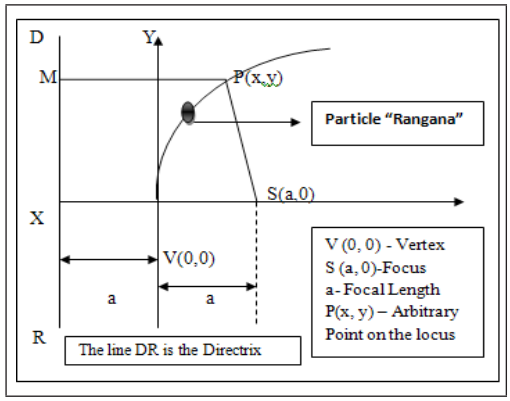

Figure 4. Representation of the path of a particle "Rangana" tracing a parabolic path which explains the recombination region.

From the Figure 4, it is evident that, when,

$$\frac{PM}{PS} = 1 \frac{PM}{PS} = 1 \quad \text{(Parabola)}$$

$$\frac{PM}{PS} > 1 \frac{PM}{PS} > 1 \quad \text{(Hyperbola)}$$

$$\frac{PM}{PS} < 1 \frac{PM}{PS} < 1 \quad \text{(Ellipse)}$$

$$\frac{PM}{PS} = 0 \frac{PM}{PS} = 0 \quad \text{(Circle)}$$

Maximum recombination occurs at low voltage; as voltage rises, more ions are created and those ions have enough energy to migrate toward the appropriate electrodes and produce an electrical signal [11]. Recombination therefore diminishes as voltage rises, and signals are produced that are graphically represented as the recombination zone in Figure 3 above. This has been taken into account that any imaginary particle "Rangana" is tracing a

parabolic route that follows the equation in order to mathematically explain this graphical representation of the recombination region. Mathematically:

$$y = f(x) = \sqrt{Ax}\,;\{O \leq x \leq B\}\text{---(a)}$$

Where the applied voltage between the electrodes is represented by the x-coordinate, the pulse amplitude is represented by the y-coordinate, and "A" is a constant. Hence, the above equation defines the locus of (x, y) co-ordinate in the graph. A locus is described as the path taken by a point when it moves in accordance with a particular rule. This indicates that the derived curve for the recombination zones adheres to a rule, or parabolic path, that is defined by the parabolic equation (a) above. The parabolic path can be mathematically represented as: for example, in the Table 1 below, the value of y can be obtained by substituting arbitrary positive values of x in the right-hand side 2Öx i.e., the equation y = 2Öx.

Table 1. Table showing the input & output values (arbitrary values).

INPUT	OUTPUT
1	2
2	2.828
3	3.464
4	4

The set of input values for a relation is called the Domain and the set of output values is called the Range. Relation is a pairing of input values with output values. It can be shown as a set of ordered pairs (x, y) where x is an input and y is an output as explained in Figure 5 below.

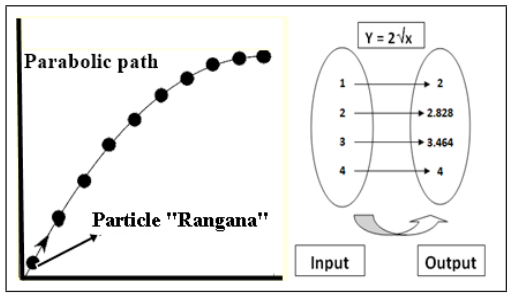

Figure 5. Representation of the parabolic function explaining the curvature described by the path of particle "Rangana".

Region BC – Saturation region:

When the voltage becomes sufficient to cause complete collection of all the charges produced i.e. negligible recombination, the above Figure 3 enters a plateau called saturation region which can be explained by the equation given below.

$$y = c\,;\{B \leq x \leq C\} \quad \text{--- (b)}$$

Where, c is a constant. This means whatever may be the value of x (applied voltage); y (pulse amplitude) remains constant which implies no recombination neither multiplication. Ionization chamber operates in this saturation region where voltage fluctuations plays negligible role [11]. Here it means that the obtained curve for the saturation region or ionization region follows a rule i.e. a constant path which is defined by the above equation or a function called constant function. The signal produced by the ionization chamber is quite weak, thus additional electronic devices are needed to obtain a good electrical signal. Additionally, as the

signal is amplified, noise level increases, which is a significant disadvantage [11]. The linear path can be mathematically represented as: for example, in Table 2 given below, the value of y which is always equal to the constant value c as represented in Figure 6 below.

Table 2. Table showing the input & output values (arbitrary values).

INPUT	OUTPUT
1	c
2	c
3	c
4	c

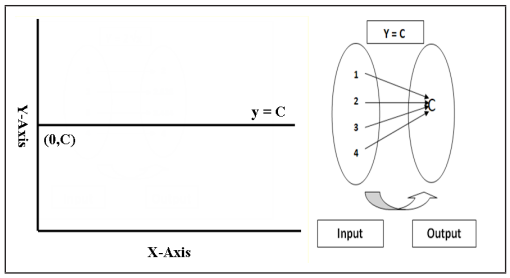

Figure 6. Representation of the Constant function explaining the straight-line path described by the path of particle "Rangana".

Region CD – Proportional region:

A proportional counter depicts a sub-critical condition where gas multiplication occurs [13] but follows a rule; for example, when voltage rises, signal amplitude rises by a fixed amount, known as the amplification factor.

Mathematically, the voltage pulse is directly proportional to the total number of charges generated because the amplification factor is constant. Therefore, it can be concluded that mathematically, voltage pulse is directly proportional to the detected photon energy. In light of this, the term "proportional counter" [13]. Proportional relationship can be mathematically represented as: for example, in the Table 3 below, the value of y can be obtained if multiplied by 4 with the corresponding value of x. It shows a one-to-one relationship & it takes the form; y = kx, where k is the constant of proportionality i.e., the equation y = 4x as shown in Figure 7 below.

Table 3. Table showing the input & output values (arbitrary values).

INPUT	OUTPUT
1	4
2	8
3	12
4	16

Hence, it is clear that the proportional region follows the function defined below which is a linear function. Mathematically,

$$y = kx, \{C \leq x \leq D\} \text{ ------ (c)}$$

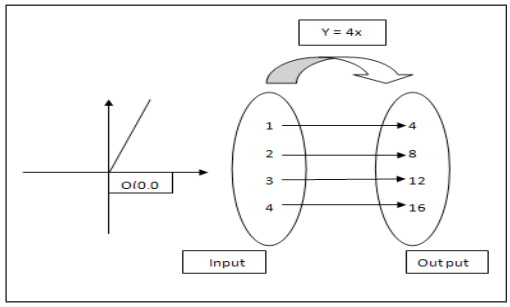

Figure 7. Representation of the linear function explaining the proportionality relation described by the path of particle "Rangana".

Region EF – Geiger Muller region:

When the voltage and electric field becomes sufficient enough to produce Geiger discharge the above curve enters a plateau called GM region which can be explained by the function called a constant function given bellow;

$$y = d; \{E \leq x \leq F\} \quad \text{---- (d)}$$

y = d (constant) means whatever may be the value in x-axis, value in y-axis remains constant. This explains that in the GM region the signal is independent of the primary ions produced and the output pulse remains constant as predicted by the path of Particle "Rangana". The linear path can be mathematically represented as: for example, in Table 4 given below, the value of y which is always equal to the constant value d as represented in Figure 8 below.

Table 4. Table showing the input & output values (arbitrary values).

INPUT	OUTPUT
1	d
2	d
3	d
4	d

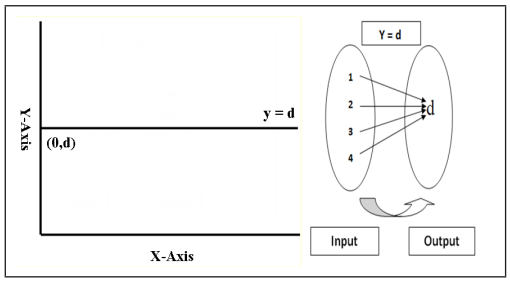

Figure 8. Representation of the constant function explaining the straight-line path described by the path of particle "Rangana".

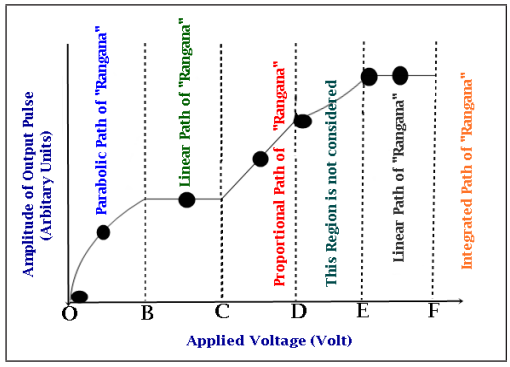

Figure 9. The schematic representation of the integrated locus of the particle "Rangana" takes the form of the characteristic curve of the gas filled detectors.

Thus, the mathematical explanation of the various regions of the gas filled detectors matches with the integrated locus of the imaginary particle "Rangana" created in the thought experiment which is pictorially demonstrated in the Figure 9 except the region of limited proportional region or non-linear region.

This study also tried to explain mathematically the cylindrical ionization chamber again considering the locus of the imaginary particle "Rangana". The increase in electric field near the anode because of the geometry of a cylindrical chamber can be expressed by using a hyperbolic function [14]. But here the electric field is constant throughout the length of the anode wire on its either side [15] as beautifully depicted in the Figure 10. Hence to represent such nature of the field a rectangular hyperbolic function is required which is given by the equation, $y = \pm b\sqrt{x^2 - a^2}/a$ $y = \pm b\sqrt{x^2 - a^2}/a$, as a=b, the equation can be written as $x^2 - y^2 = a^2$ $x^2 - y^2 = a^2$.

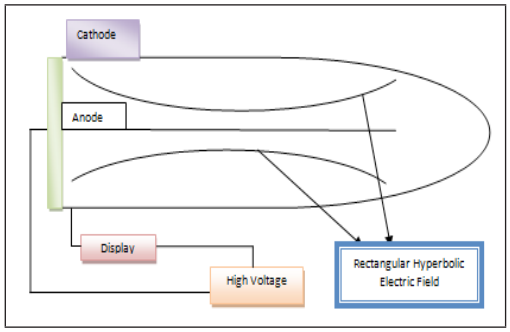

Figure 10. Pictorial Representation of the concept of detection of radiation in a cylindrical chamber showing the hyperbolic electrical field based on the locus of "Rangana".

3. RESULTS AND DISCUSSION

This study revealed a simple and abstract way of explaining the characteristic curve of the gas-filled detectors based on a thought experiment which successfully compared and the locus of a hypothetical particle "Rangana" in order to offer a fresh viewpoint. In this study the recombination region was described by a parabolic function, the ionization and Geiger regions by constant functions and the proportional region by a linear function. A rectangular hyperbolic function was used to describe the electric field in a cylindrical chamber in addition to the explanation of the characteristic curve. Other mathematical techniques can also be tried in future. Since the region of limited proportionality is not necessary for the dosimetry requirement in the field of radiation oncology and is also not necessary for the purpose of radiation survey in any installation where radioactive sources or radiation generating machines were used. Thus, the mathematical explanation of the region of limited proportionality was not attempted here. But the limited proportional region which was not described here can be tried using a suitable non linear function or any other mathematical techniques.

4. CONCLUSION

In accordance with our prediction, the characteristic curve was uniquely explained by the triptychs of gas-filled detectors, a thought experiment and various mathematical functions based on the movement of the imagined particle "Rangana". Thus, adding a new dimension to the explanation of the gas filled detectors.

ACKNOWLEDGEMENTS

We express our most sincere gratitude to the Director Dr. B. C. Goswami and Superintendent, Dr. Devajit Choudhury; State Cancer Institute, Gauhati Medical College, Guwahati, Assam, India for their continuous guidance and encouragement. We also express our most sincere gratitude to Mrs. Tania Sen and Miss Ritvika Bhattacharjee (Curie) for their encouragement.

REFERENCES

[1] Damle, S. G. (2014). Curiosity: The greatest virtue of man. *Contemporary Clinical Dentistry*, *5*(2), 147-148.

[2] Weinberg, S. (2011). Dreams of a final theory: The scientist's search for the ultimate laws of nature. *Vintage.*

[3] Arifiyanti, S. F., & Wahyuningish, S.

(2015). Using Integrated Analogy in Physics Education to Building Concept of Representation: The Way to be Great Inventor. In *Proceeding of International Conference on Research, Implementation and Education of Mathematics and Science*.

[4] Tilton, H. B. (1996). The hydrogen atom: The Rutherford model. In *Models and modelers of hydrogen* 33-47.

[5] Assis, A. K. T., Wiederkehr, K. H., & Wolfschmidt, G. (2011). *Weber's planetary model of the atom*. Hamburg: Tredition Science.

[6] Lee, E., Farrelly, D., & Uzer, T. (1997). A Saturnian atom. *Optics Express*, *1*(7), 221-228.

[7] Yagi, E. (1972). The Development of Nagaoka's Saturnian Atomic Model II (1904-05)." *Japanese Studies in the History of Science*, *11*, 73-89.

[8] Das, A., & Ferbel, T. (2003). *Introduction to nuclear and particle physics*. World Scientific, 53-72.

[9] Britannica, T. Editors of Encyclopaedia (2016, April 22). *Optical model*. *Encyclopedia Britannica*. Accessed 27th August 2022 https://www.britannica.com/science/optical-model.

[10] Johnson, K. E. (2004). From natural history to the nuclear shell model: Chemical thinking in the work of Mayer, Haxel, Jensen, and Suess. *Physics in Perspective*, *6*(3), 295-309.

[11] Sorenson, J. A., Phelps, M. E. (1980). *Physics in Nuclear Medicine.* Grune & Stratton, Inc., 49-60.

[12] Ahmed, S. N. (2007). *Physics and engineering of radiation detection*. Academic Press, 149-216.

[13] Knoll, G. F. (2000). *Radiation Detection and Measurement*. John Wiley & sons, Inc., 129-155, 159-163, 201-204.

[14] Sharpe, J. (1955). *Nuclear Radiation Detectors.* London: Methuen & Co. Ltd. New York: John Wiley & sons, INC., 6-7, 145-149.

[15] Leo, W. R. (1993). *Techniques for Nuclear and Particle Physics Experiments*. Springer International Student Edition; New Delhi: Narosa Publishing House., 128-133, 137-139.

Research article:

KF-Al_2O_3 catalyzed One-Pot Synthesis of Benzo[α]xanthene-11-ones

Iadeishisha Kharbangar*

Department of Chemistry, St. Edmund's College, Shillong, Meghalaya, India

Article Info:
https://doi.org/10.54290/spect/2022.v9.1.0002

Received: July 30th, 2022
Revised: September 20th, 2022
Accepted: October 1st, 2022

Corresponding author:
iadeik@gmail.com

Abstract: KF-Al_2O_3 as a recyclable basic catalyst for the one-pot synthesis of benzoxanthenone derivatives by the reaction of aromatic aldehydes, *β*-naphthol and dimedone in the presence of a catalyst in ethanol under microwave irradiation. The protocol is environmentally benign, offering access to a range of benzoxanthenone derivaties in good to excellent yields.

Keywords: *KF-Al_2O_3; Benzoxanthenone; Microwave Irradiation; Ethanol; One-pot synthesis.*

1. INTRODUCTION

Benzoxanthenones, compounds containing a xanthene skeleton are important biologically active compounds which are known to possess analgesic [1], antiviral [2], antibacterial[3] and anti-inflammatory properties [4]. These compounds have also been established as antagonists for paralyzing the action of zoxazolamine [5] and in photodynamic therapy [6]. Furthermore, these heterocyclic compounds have found applications in industries such as fluorescent dyes [7], in laser technology [8] and as pH sensitive fluorescent materials for visualization of biomolecules [9]. Their broad utility range have made these xanthene scaffolds synthetic targets, thereby, increasing the need to devise and design newer synthetic routes for exploitation of these structural moieties. Therefore, their synthesis occupies as a subject of immense interest to synthetic chemists and has achieved prominence in synthetic, organic as well as medicinal chemistry.

The general strategy to synthesize xanthenone scaffolds involves the multi-component condensation of aromatic aldehydes, *β*-naphthol and cyclic 1,3-dicarbonyl compounds such

How to Cite:
Kharbangar I.(2022). KF-Al2O3 catalyzed One-Pot Synthesis of Benzo[α]xanthene-11-ones. *Spectrum: Science and Technology, v9 (1), 11-24.* https://doi.org/10.54290/spect/2022.v9.1.0002

as dimedone or cyclohexanedione in the presence of a catalyst or reagent. Several catalysts [10-29] have been established in affecting this synthesis. Although these synthetic strategies have their own advantage and are quite useful, they are often confronted with drawbacks such as harsh reaction conditions, laborious work-ups, expensive catalysts and the use of toxic organic solvents. Steering clear of these limitations has inspired to develop an efficient method involving catalytic recyclability, simple work-up procedure and the use of non-toxic organic solvents for the preparation of benzoxanthenone and its derivatives under mild and practical conditions. Because of the growing interest in faster, greener organic reactions, microwave irradiation has come out as an attractive technology and has been successfully exploited in carrying out many synthetic organic reactions both in solvent and solvent-free conditions [30]. While microwave irradiation has remarkably reduced reaction times, it has also been a source which enhances the product yields and product purities by reducing unwanted side reactions compared to the same chemistry using conventional heating methods [31].

KF-Al_2O_3 has emerged as a versatile solid-support catalyst in organic syntheses, the applications of which have offered many advantages including mild reaction conditions, cleaner reactions, shorter reaction times, lower catalyst loading, ease of handling and especially catalyst recyclability. The use of microwave technology in combination with solid-support catalysts is productive to a chemist by providing ease of workup procedure by simple filtration and that the combinations of supported reagents can be added without interaction between them. Hence, the importance to develop such methods for sustainable chemistry is of great importance to synthetic organic chemists.

2. EXPERIMENTAL

In continuation of our work to explore newer methodologies for the synthesis of heterocycles [32], we wish to report herein a one-pot reaction of aromatic aldehydes (1), *β*-naphthol (2) and dimedone (3) in the presence of KF-Al_2O_3 as catalyst in ethanol under microwave to afford the benzoxanthenones (4) (Scheme 1). Non-usage of organic solvents in these reactions in organic synthesis gives way to a clean, efficient, practical and economical/cost-effective technology due to the increased safety, simplicity of work-up and cost reduction.

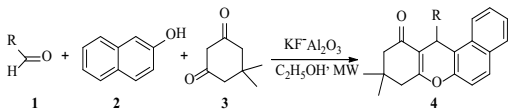

Scheme 1: Three-component synthesis of benzoxanthenone derivatives

All the melting points were taken by open capillary method and were uncorrected. The ^1H and ^{13}C NMR were recorded on Bruker AVANCE II 400 and Bruker Av III HD-300 MHz FT-NMR spectrometer with tetramethylsilane (TMS) as the internal standard using $CDCl_3$ and $(CD_3)_2SO$ as the solvents.

The infra-red (IR) spectra were obtained using Perkin-Elmer FT-IR spectrophotometer. The mass spectra were recorded on Waters ZQ-4000 equipped with ESI and API mass detector. The Carbon, Hydrogen and Nitrogen (CHN) analysis was done on Perkin-Elmer PE 2400 Series II machine. The thin layer chromatography (TLC) was performed using the Merck were visualized under iodine chamber or by precoated TLC plates and the components exposure or by the acidic potassium permanganate ($KMnO_4$) spray technique. All the chemicals and reagents obtained commercially were used directly without further purification as otherwise prepared according to standard literature procedures.

Solvents were dried prior to use following standard procedures in the literature.

2.1 General experimental procedure for the preparation of Benzo[α] xanthene-11-ones:

KF-Al_2O_3 (10 mol%) was added to a mixture of aldehyde (1), (1 mmol), *β*-naphthol (2) (1 mmol) and dimedone (3) (1 mmol) in ethanol (2 mL). The reaction was reacted under microwave irradiation for 15 - 25 minutes. On completion of the reaction (monitored by thin layer chromatography), the catalyst was separated from the reaction mixture by filtration through a celite bed and thoroughly washed with ethyl acetate. The combined organic extract was removed by evaporation under reduced pressure and the resulting benzoxanthenone derivatives (4) were obtained in pure form after column chromatography on silica gel using ethyl acetate-hexane as eluent.

3. RESULTS AND DISCUSSION

4-Chlorobenzaldehyde (1e), *β*-naphthol (2) and dimedone (3) were selected as the representative substrates to investigate the reaction conditions. In an initial endeavour, a mixture of 4-chlorobenzaldehyde (1e) (1.00 mmol), *β*-naphthol (2) (1.00 mmol) and dimedone (3) (1.00 mmol) in ethanol was heated at 40°C in the presence of KF-Al_2O_3 (30 mol%) for 24 h and the desired product, 12-(4-chlorophenyl)-9,9-dimethyl-9,10-dihydro-8*H*-benzo[*α*] xanthen-11(12*H*)-one (4e), was obtained in 56% yield (entry 1, Table 1). In the next set, on refluxing the equivalent reaction mixture for 24 hours, the product 4e resulted with a fair yield of 79% (entry 2, Table 1). On the other hand, when the reaction was executed under microwave in the presence of KF-Al_2O_3 (10mg, 5 mol%) in ethanol for 10 minutes, the desired product 4e increased to a higher yield of 87% (entry 3, Table 1). On further optimization of the catalyst load, it was found that the use of 10 mol% of KF-Al_2O_3 was optimal which produced 4e with maximum yield of 92% in 20 minutes (entry 4, Table 1) and further increasing the load of catalyst did not give a better yield of the product.

Table 1: Optimization of the catalyst with product 4e.

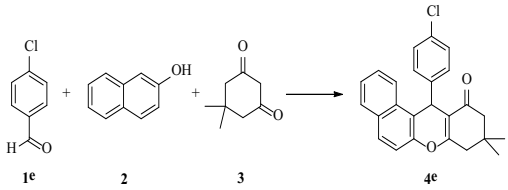

Entry	Reaction Conditions	Time	Yield[a] (%)
1	KF-Al_2O_3 (30 mol%), EtOH, heat	24h	56
2	KF-Al_2O_3 (30 mol%), EtOH, reflux	24h	79
3	KF-Al_2O_3 (5 mol%), EtOH, MW	10 mins	87
4	KF-Al_2O_3 (10 mol%), EtOH, MW	20 mins	92

[a]Isolated Yield

To investigate the feasibility of reuse of the catalyst, the KF-Al_2O_3 which is obtained after filtration from the previous reaction was thoroughly washed with ethyl acetate, dried and reused for the reaction of 4-chlorobenzaldehyde (1e), *β*-naphthol (2) anddimedone (3). The reaction could satisfactorily furnish the product 12-(4-chlorophenyl)-9, 9-dimethyl-9, 10-dihydro-8*H*-benzo[*α*]xanthen-11(12*H*)-one (4e) with 89% yield. The recyclability of the catalyst was further established when it was found to show good activity even after the fourth run without substantial drops in the product yield (Table 2).

Table 2: Recyclability results of KF-Al_2O_3 with 4e.

Entry	Reaction Conditions	Time (mins)	Yield[a] (%)
1	KF-Al_2O_3 (recycled once), EtOH	25	89
2	KF-Al_2O_3 (recycled twice), EtOH	25	84
3	KF-Al_2O_3 (recycled thrice), EtOH	30	79[b]
4	KF-Al_2O_3 (recycled four times), EtOH	40	76[b]

[a]Isolated yield. [b]Purified by chromatography

Aided by these results, different substituted aromatic aldehydes were engaged and a series of 12-aryl-9,9-dimethyl-9,10-dihydro-8*H*-enzo[*α*] xanthen-11(12*H*)-ones (4) was prepared under the optimized reaction conditions (Table 3). Without taking account of the presence of electron-donating or electron-withdrawing groups on the *ortho*-, *meta*- or *para*-positions of the ring of the aromatic aldehyde, all reactions proceeded smoothly and afforded the corresponding products in good to excellent yields (entries 4a - o, Table 3) in 15 - 25 minutes. Halogen-substituted aldehydes participated very well and reacted with *β*-naphthol (2) and dimedone (3) to afford the desired products in 15 - 25 minutes with excellent yields (entries 4b - f, Table 3, 85 - 92%). The reactions involving aldehydes bearing hydroxyl or nitro groups also proceeded smoothly and furnished their corresponding

benzoxanthenones (entries 4g - j, Table 3, 78 - 89%). Even unsubstituted or other aldehydes bearing cyano, methoxy and methyl groups also underwent reactions efficiently with (2) and (3) and gave the corresponding products in high yields (entries, 4a, 4k-m, Table 3). The present method was also extended to disubstituted aldehydes such as 4-hydroxy-3-methoxybenzaldehyde (1n) and 3,4-dihydroxybenzaldehyde (1o) and their reaction with (2) and (3) availed the products (4n) and (4o) with 68-70% yield respectively.

The mechanistic route for the benzo[α]xanthen-11-one derivatives (4) is believed to proceed through the formation of the intermediate (5), by the nucleophilic addition of β-naphthol (2) to the protonated aldehyde (1) catalyzed by KF-Al_2O_3. Subsequent Michael addition of dimedone (3) to the *in situ* formed intermediate (5) afforded the cyclic hemiketal (6) which on dehydration gave the product 4 (Scheme 2).

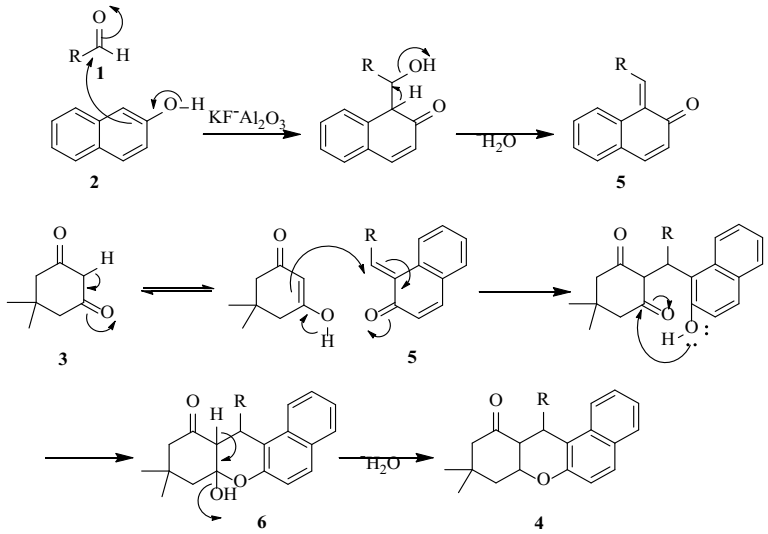

Table 3: Three-component synthesis of Benzo[α]xanthen-11-one derivatives.

Entry	Substrate (1)	Time (mins)	Product (4)[c]	Yield[a] (%)
1	C_6H_5 (1a)	20	4a	89
2	3-BrC_6H_4 (1b)	25	4b	85[b]
3	4-BrC_6H_4 (1c)	15	4c	88
4	2-ClC_6H_4 (1d)	20	4d	87[b]
5	4-ClC_6H_4 (1e)	20	4e	92
6	4-FC_6H_4 (1f)	25	4f	90
7	2-OHC_6H_4 (1g)	20	4g	81[b]
8	4-HOC_6H_4 (1h)	20	4h	78[b]
9	3-$NO_2C_6H_4$ (1i)	20	4i	89[b]

10	4-$NO_2C_6H_4$ (1j)	20	4j	86[b]
11	3-NCC_6H_4 (1k)	25	4k	70
12	4-$CH_3OC_6H_4$ (1l)	20	4l	82[b]
13	4-$CH_3C_6H_4$ (1m)	20	4m	85[b]
14	4-OH-3-$CH_3OC_6H_3$ (1n)	25	4n	68[b]
15	3,4-$(HO)_2C_6H_3$ (1o)	25	4o	70[b]

[a]Isolated yield. [b]Purified by column chromatography.[c]Structure shown in Fig. 1.

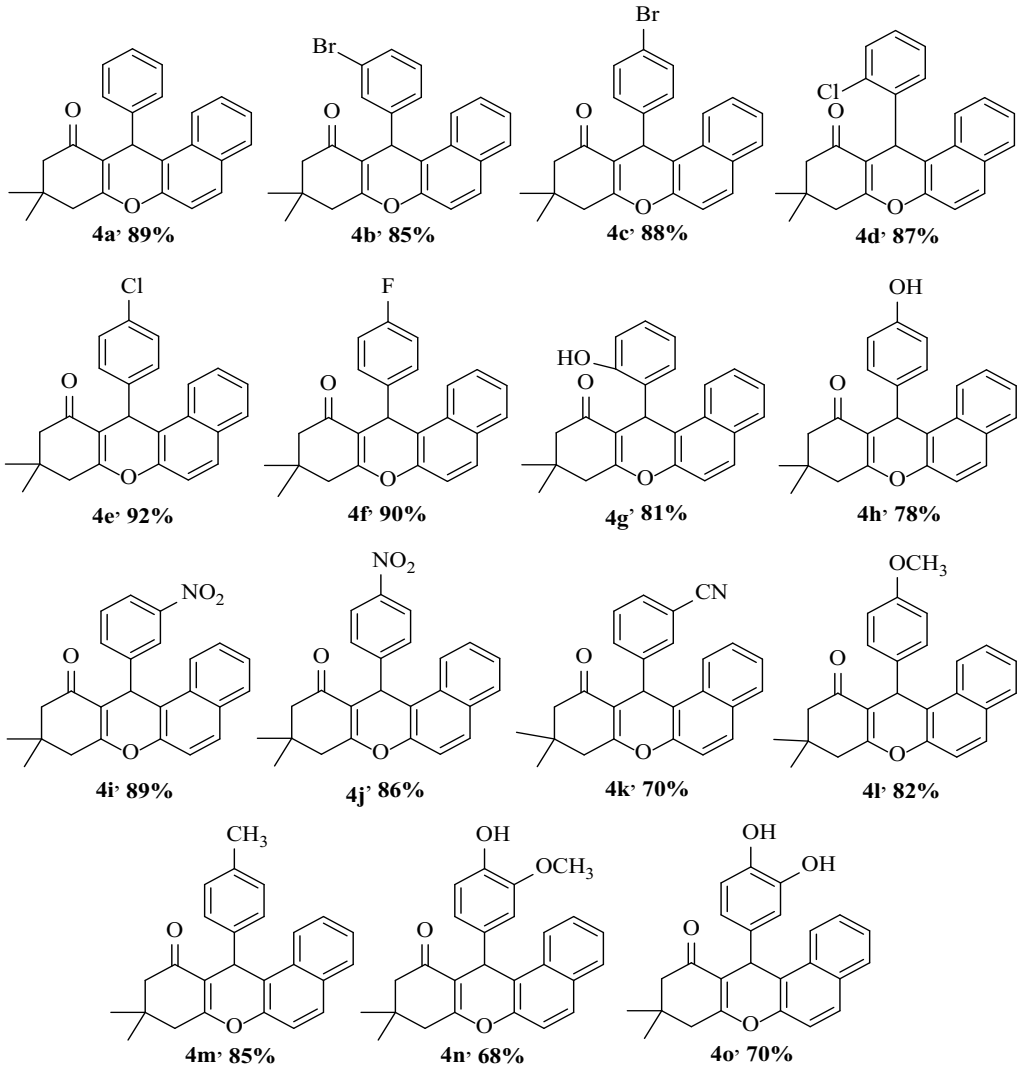

Figure 1: Synthesized Benzo[α]xanthene-11ones

3.1 Spectroscopic data:

The synthesized products were characterized from their ^{1}HNMR, ^{13}C NMR, FT-IR and MS analyses.

9,9-dimethyl-12-phenyl-9,10-dihydro-8*H*-benzo[*α*]xanthen-11(12*H*)-one (4a)mp 150°C - 152°C; ^{1}H NMR ($CDCl_3$, 400 MHz): *δ* 1.01 (s, 3H), 1.08 (s, 3H), 2.12 (d, *J* = 12.8 Hz, 1H), 2.20 (d, *J* = 16.4 Hz, 1H), 2.28 (s, 2H), 5.79 (s, 1H), 6.29 (t, *J* = 14.8 Hz, 1H), 6.49 (d, *J* = 7.6 Hz, 1H), 6.67 (d, *J* = 10.8 Hz, 1H), 6.70-7.08 (m, 5H), 7.37-7.52 (m, 2H), 7.72-7.78 (m, 1H) ppm; ^{13}C NMR ($CDCl_3$, 100 MHz): *δ* 27.0, 31.3, 37.1, 42.1, 49.4, 106.4, 118.0, 122.9, 123.3, 124.9, 125.4, 126.9, 127.8, 128.0, 128.2, 129.4, 133.9, 144.5, 151.4, 163.4, 196.6 ppm; IR (KBr): 1054, 1149, 1228, 1374, 1602, 2957, 3062 cm^{-1}; Mass (ES+) calcd. for $C_{25}H_{25}O_2$ 354.4; found m/z 355.8 $[M + H]^+]^+$; Anal. calcd. for $C_{25}H_{25}O_2$: C, 84.72; H, 6.26 %; found: C, 84.69; H, 6.22 %.

12-(3-bromophenyl)-9,9-dimethyl-9,10-dihydro-8*H*-benzo[*α*]xanthen-11(12*H*)-one (4b) mp 166°C - 170°C; ^{1}H NMR ($CDCl_3$, 400 MHz): *δ* 1.17 (s, 3H), 1.26 (s, 3H), 2.32 (d, *J* = 16.8 Hz, 1H), 2.43 (d, *J* = 17.6 Hz, 1H), 2.66 (s, 2H), 5.76 (s, 1H), 6.93 (d, *J* = 7.2 Hz, 1H), 7.00-7.19 (m, 5H), 7.41 (d, *J* = 7.2 Hz, 1H), 7.53 (s, 1H), 7.61 (t, *J* = 7.6 Hz, 1H), 7.79 (d, *J* = 8.4 Hz, 1H) ppm; ^{13}C NMR ($CDCl_3$, 100 MHz): *δ* 27.7, 28.7, 37.8, 43.2, 50.7, 121.8, 124.2, 126.1, 126.4, 126.6, 126.7, 127.2, 127.4, 129.7, 130.0, 130.3, 130.5, 130.8, 131.7, 131.8, 196.8 ppm; IR (KBr): 764, 1055, 1118, 1228, 1373, 1471, 1649, 2958, 3068 cm^{-1}; Mass (ES+) calcd. for $C_{25}H_{21}BrO_2$ 433.3; found m/z 456.0 $[M + Na]^+]^+$; Anal. calcd. for $C_{25}H_{21}BrO_2$: C, 69.29; H, 4.88 %; found: C, 69.58; H, 4.75 %.

12-(4-bromophenyl)-9,9-dimethyl-9,10-dihydro-8*H*-benzo[*α*]xanthen-11(12*H*)-one (4c) mp 186°C - 188°C; ^{1}H NMR ($CDCl_3$, 400 MHz): *δ* 0.97 (s, 3H), 1.09 (s, 3H), 2.10 (d, *J* = 17.6 Hz, 1H), 2.31 (d, *J* = 17.6 Hz, 1H), 2.57 (s, 2H), 5.93 (s, 1H), 6.80-6.87 (m, 4H), 7.21 (t, *J* = 8.4 Hz, 1H), 7.30 (d, *J* = 8.4 Hz, 1H), 7.44 (t, *J* = 7.6 Hz, 1H), 7.54 (t, *J* = 8.0 Hz, 1H), 7.71 (d, *J* = 8.4 Hz, 1H), 8.23 (d, *J* = 8.4 Hz, 1H) ppm; ^{13}C NMR ($CDCl_3$, 100 MHz): *δ* 31.8, 36.1, 38.0, 42.2, 51.4, 103.8, 119.7, 123.9, 124.4, 124.7, 124.9, 126.5, 129.9, 130.7, 132.1, 133.4, 148.2, 150.7, 194.3 ppm; IR (KBr): 798, 1011, 1145, 1370, 1604, 1655, 2887, 2960 cm^{-1}; Mass (ES+) calcd. for $C_{25}H_{21}BrO_2$ 433.3; found m/z 434.1 $[M + H]^+]^+$; Anal. calcd. for $C_{25}H_{21}BrO_2$: C, 69.29; H, 4.88 %; found: C, 69.45; H, 4.63 %.

12-(2-chlorophenyl)-9,9-dimethyl-9,10-dihydro-8*H*-benzo[*α*]xanthen-11(12*H*)-one (4d)mp 180°C - 182°C; ^{1}H NMR ($CDCl_3$, 300 MHz):*δ* 0.95 (s, 3H), 1.06 (s, 3H), 2.02 (d, *J* = 14.1 Hz, 1H), 2.43 (d, *J* = 14.1 Hz, 1H), 2.52 (s, 2H), 5.62 (s, 1H), 7.06-7.24 (m, 5H), 7.28-7.31 (m, 3H), 7.35-7.39 (m, 2H) ppm; ^{13}C NMR ($CDCl_3$, 100 MHz):*δ* 27.8, 31.8, 32.3, 42.4 50.4, 100.6, 109.2, 114.6, 125.2, 125.8, 126.4, 128.4, 129.0, 129.4, 130.2, 132.3, 132.8, 137.4, 140.1, 167.1, 187.8, 195.6 ppm; IR (KBr): 745, 1072, 1230, 1383, 1610, 1641, 2957, 3065 cm^{-1}; Mass (ES+) calcd. for $C_{25}H_{21}ClO_2$ 388.8; found m/z 389.8 $[M + H]^+]^+$; Anal. calcd. for

$C_{25}H_{21}ClO_2$: C, 77.21; H, 5.44 %; found: C, 77.25; H, 5.42 %.

12-(4-chlorophenyl)-9,9-dimethyl-9,10-dihydro-8*H*-benzo[*α*]xanthen-11(12*H*)-one (4e) mp 186°C - 188°C; ^{1}H NMR ($CDCl_3$, 400 MHz): *δ* 1.01 (s, 3H), 1.09 (s, 3H), 2.19 (d, *J* = 16.0 Hz, 1H), 2.26 (d, *J* = 16.4 Hz, 1H), 2.64 (s, 2H), 5.05 (s, 1H,), 7.03 (d, *J* = 8.4 Hz, 1H), 7.10-7.16 (m, 3H), 7.43-7.46 (m, 3H), 7.51 (t, *J* = 7.6 Hz, 1H), 7.71 (d, *J* = 8.0 Hz, 1H), 8.19 (d, *J* = 8.0 Hz, 1H) ppm; ^{13}C NMR ($CDCl_3$, 100 MHz): *δ* 27.5, 32.3, 37.9, 41.5, 50.8, 113.3, 119.2, 121.1, 123.7, 124.7, 126.5, 126.8, 127.7, 128.5, 129.6, 132.2, 133.2, 144.1, 144.3, 164.3, 197.0 ppm; IR (KBr): 1052, 1176, 1227, 1370, 1646, 2960, 3049 cm^{-1}; Mass (ES+) calcd. for $C_{25}H_{21}ClO_2$ 388.8; found m/z 389.8 $[M + H]^+]^+$; Anal. calcd. for $C_{25}H_{21}ClO_2$: C, 77.21; H, 5.44 %; found: C, 77.22; H, 5.42 %.

12-(4-fluorophenyl)-9,9-dimethyl-9,10-dihydro-8*H*-benzo[*α*]xanthen-11(12*H*)-one (4f) mp 185°C - 187°C; ^{1}H NMR ($CDCl_3$, 400 MHz): *δ* 0.98 (s, 3H), 1.18 (s, 3H), 2.11-2.32 (m, 4H), 6.22 (s, 1H), 6.55 (d, *J* = 7.6 Hz, 1H), 6.66 (d, *J* = 7.2 Hz, 1H), 6.97 (t, *J* = 8.4 Hz, 1H), 7.14-7.19 (m, 4H), 7.46 (t, *J* = 6.8 Hz, 1H), 7.75 (d, *J* = 8.0 Hz, 1H), 8.19 (d, *J* = 8.0 Hz, 1H) ppm; ^{13}C NMR ($CDCl_3$, 100 MHz): *δ* 28.6, 30.8, 39.9, 106.4, 114.5, 114.7, 121.7, 122.8, 124.5, 124.7, 124.8, 126.3, 129.6, 131.7, 135.7, 151.3, 159.5, 161.9 ppm; IR (KBr): 838, 1026, 1155, 1256, 1369, 1505, 1587, 1601, 2959, 3068 cm^{-1}; Mass (ES+) calcd. for $C_{25}H_{21}FO_2$372.1; found m/z 373.4 $[M + H]^+]^+$; Anal. calcd. for $C_{25}H_{21}FO_2$: C, 80.62; H, 5.10 %; found: C, 81.03; H, 5.06 %.

12-(2-hydroxyphenyl)-9,9-dimethyl-9,10-dihydro-8*H*-benzo[*α*]xanthen-11(12*H*)-one (4g) mp 208°C - 210°C; ^{1}H NMR ($CDCl_3$, 400 MHz): *δ* 1.18 (s, 3H), 1.25 (s, 3H), 2.13 (d, *J* = 12.4 Hz, 1H), 2.40 (d, *J* = 11.2 Hz, 2H), 2.59 (s, 2H), 5.60 (s, 1H), 6.73 (d, *J* = 8.0 Hz, 1H), 6.87 (d, *J* = 8.8 Hz, 1H), 7.07 (d, *J* = 7.6 Hz, 1H), 7.23 (d, *J* = 8.4 Hz, 1H), 7.41-7.46 (m, 4H), 7.69 (d, *J* = 7.2 Hz, 1H), 8.24 (d, *J* = 8.0 Hz, 1H), 8.57 (s, 1H) ppm; ^{13}C NMR ($CDCl_3$, 100 MHz): *δ* 28.5, 32.4, 35.9, 47.8, 54.1, 114.2, 118.9, 119.9, 120.7, 123.5, 124.0, 124.6, 126.3, 126.6, 126.9, 127.9, 129.7, 131.9, 133.7, 144.7, 154.6, 204.5 ppm; IR (KBr): 1000, 1171, 1256, 1380, 1516, 1574, 1616, 1705, 2967, 3021 cm^{-1}; Mass (ES+) calcd. for $C_{25}H_{22}O_3$ 370.4; found m/z 371.1 $[M + H]^+]^+$; Anal. calcd. for $C_{25}H_{22}O_3$: C, 81.06; H, 5.99 %; found: C, 81.56; H, 5.79 %.

12-(4-hydroxyphenyl)-9,9-dimethyl-9,10-dihydro-8*H*-benzo[*α*]xanthen-11(12*H*)-one (4h) mp 224°C - 226°C; ^{1}H NMR ($CDCl_3$, 300 MHz): *δ* 1.09 (s, 3H), 1.15 (s, 3H), 2.27 (d, *J* = 16.5 Hz, 1H), 2.34 (d, *J* = 16.2 Hz, 1H), 2.63 (s, 2H), 4.77 (s, 1H), 5.06 (s, 1H), 6.62 (d, *J* = 8.4 Hz, 1H), 7.09-7.15 (m, 4H), 7.47-7.59 (m, 3H), 7.77 (d, *J* = 8.1 Hz, 1H), 8.25 (d, *J* = 8.4 Hz, 1H) ppm; ^{13}C NMR ($CDCl_3$, 100 MHz): *δ* 28.2, 31.2, 36.4, 40.5, 49.9, 112.8, 114.3, 119.3, 119.9, 122.6, 123.3, 125.2, 126.1, 126.6, 128.0, 131.9, 136.0, 142.8, 154.5, 163.0, 196.1 ppm; IR (KBr): 1057, 1178, 1228, 1370, 1574, 1625, 2958, 3409 cm^{-1}; Mass (ES+) calcd. for $C_{25}H_{22}O_3$ 370.4; found m/z 371.0 $[M + H]^+]^+$; Anal. calcd. for $C_{25}H_{22}O_3$: C, 81.06; H, 5.99 %; found: C, 81.43; H, 5.85 %.

9,9-dimethyl-12-(3-nitrophenyl)-9,10-dihydro-8*H*-benzo[*α*]xanthen-11(12*H*)-one (4i) mp 169°C - 171°C; ^{1}H NMR ($CDCl_3$, 300 MHz): *δ* 1.10 (s, 3H), 1.18 (s, 3H), 1.68 (s, 2H), 2.26 (d, *J* = 16.5 Hz, 1H), 2.35 (d, *J* = 16.2 Hz, 2H), 5.26 (s, 1H), 7.09 (d, *J* = 8.7 Hz, 1H), 7.41 (t, *J* = 7.8 Hz, 1H), 7.52-7.63 (m, 3H), 7.69 (d, *J* = 7.8 Hz, 1H), 7.79 (d, *J* = 7.8 Hz, 1H), 7.98-8.02 (m, 1H), 8.11 (s, 1H), 8.29 (d, *J* = 8.1 Hz, 1H) ppm; ^{13}C NMR ($CDCl_3$, 100 MHz): *δ* 27.5, 38.3, 41.5, 50.7, 112.5, 118.1, 121.1, 121.7, 123.0, 123.7, 125.0, 126.4, 126.7, 126.8, 127.7, 129.2, 133.3, 134.5, 144.1, 147.8, 148.4, 196.9 ppm; IR (KBr): 808, 1052, 1177, 1225, 1370, 1473, 1528, 1655, 2960, 3058 cm^{-1}; Mass (ES+) calcd. for $C_{25}H_{21}NO_4$ 399.4; found m/z 400.1 $[M + H]^+]^+$; Anal. calcd. for $C_{25}H_{21}NO_4$: C, 75.17; H, 5.30; N, 3.51 %; found: C, 75.24; H, 5.26; N, 3.47 %.

9,9-dimethyl-12-(4-nitrophenyl)-9,10-dihydro-8*H*-benzo[*α*]xanthen-11(12*H*)-one (4j) mp 179°C - 182°C**;** ^{1}H NMR ($CDCl_3$, 300 MHz): *δ* 1.03 (s, 3H), 1.24 (s, 3H), 2.38 (d, *J* = 11.1 Hz, 1H), 2.45 (d, *J* = 12.3 Hz, 1H), 2.53 (s, 2H), 5.55 (s, 1H), 6.71 (d, *J* = 8.7 Hz, 1H), 7.23-7.33 (m, 5H), 7.46-7.51 (m, 1H), 8.14 (d, *J* = 8.7 Hz, 1H), 8.18-8.22 (m, 2H) ppm; ^{13}C NMR ($CDCl_3$, 100 MHz): *δ* 28.4, 32.2, 36.9, 45.3, 53.7, 113.8, 120.2, 122.5, 124.7, 125.3, 126.0, 126.6, 129.9, 132.3, 125.5, 188.6, 189.9 ppm; IR (KBr): 852, 1065, 1167, 1252, 1375, 1512, 2959, 3063 cm^{-1}; Mass (ES+) calcd. for $C_{25}H_{21}NO_4$ 399.4; found m/z 400.3 $[M + H]^+]^+$; Anal. calcd. for $C_{25}H_{21}NO_4$: C, 75.17; H, 5.30; N, 3.51 %; found: C, 75.09; H, 5.33; N, 3.49 %.

3-(9,9-dimethyl-11-oxo-9,10,11,12-tetrahydro-8*H*-benzo[*α*]xanthen-12-yl) benzonitrile (4k) mp 190°C - 193°C; ^{1}H NMR ($CDCl_3$, 300 MHz): *δ* 1.20 (s, 3H), 1.22 (s, 3H), 2.23 (d, *J* = 12.9 Hz, 1H), 2.40 (d, *J* = 12.9 Hz, 1H), 2.50 (s, 2H), 5.30 (s, 1H), 6.72 (d, *J* = 8.4 Hz, 1H), 7.31-7.41 (m, 2H), 7.46-7.61 (m, 5H), 7.73-7.77 (m, 1H), 8.18-8.21 (m, 1H) ppm; ^{13}C NMR ($CDCl_3$, 100 MHz): *δ* 31.8, 38.0, 42.6, 53.5, 59.6, 103.8, 116.7, 123.6, 123.7, 125.1, 126.6, 130.1, 130.8, 132.1, 133.8, 134.9, 137.9, 138.2, 139.5, 150.7, 210.0 ppm; IR (KBr): 1061, 1177, 1266, 1390, 1575, 1719, 2245, 2961, 3056 cm^{-1}; Mass (ES+) calcd. for $C_{26}H_{21}NO_2$ 379.4; found m/z 380.0 $[M + H]^+]^+$; Anal. cacld. for $C_{26}H_{21}NO_2$: C, 82.30; H, 5.58; N, 3.69 %; found: C, 82.56; H, 5.48; N, 3.89 %.

12-(4-methoxyphenyl)-9,9-dimethyl-9,10-dihydro-8*H*-benzo[*α*]xanthen-11(12*H*)-one (4l) mp 201°C - 204°C; ^{1}H NMR ($CDCl_3$, 300 MHz): *δ* 1.03 (s, 3H), 1.08 (s, 3H), 2.17 (d, *J* = 17.4 Hz, 1H), 2.34 (d, *J* = 17.1 Hz, 1H), 2.53 (s, 2H), 3.80 (s, 3H), 5.30 (s, 1H), 6.23-6.29 (m, 1H), 6.39-6.42 (m, 1H), 6.62 (d, *J* = 7.8 Hz, 1H), 6.80 (d, *J* = 7.8 Hz, 1H), 6.88 (d, *J* = 8.7 Hz, 1H), 7.14 (d, *J* = 8.7 Hz, 1H), 7.45-7.53 (m, 2H), 7.83 (d, *J* = 8.4 Hz, 1H), 8.24 (d, *J* = 8.1 Hz, 1H) ppm; ^{13}C NMR ($CDCl_3$, 100 MHz): *δ* 28.0, 31.8, 36.6, 43.1, 50.8, 55.2, 113.7, 114.3, 116.7, 122.7, 124.0, 125.6, 125.7, 127.0, 129.0, 130.0, 133.1, 135.7, 152.2, 158.4 ppm; IR (KBr): 1033, 1176, 1248, 1375, 1607, 2957, 3070 cm^{-1}; Mass (ES+) calcd. for $C_{26}H_{24}O_3$ 384.4; found m/z 385.1 $[M + H]^+]^+$; Anal. calcd. for $C_{26}H_{24}O_3$: C, 81.22; H, 6.29 %; found: C, 81.35; H, 6.24 %.

9,9-dimethyl-12-(*p*-tolyl)-9,10-dihydro-8*H*-benzo[*α*]xanthen-11(12*H*)-one (4m) mp 177°C - 179°C; ^{1}H NMR ($CDCl_3$, 300MHz): *δ* 1.09 (s, 3H), 1.20 (s, 3H), 2.31 (s, 2H), 2.40 (d, *J* = 12.6 Hz, 1H), 2.50 (d, *J* = 14.4 Hz, 1H), 2.62 (s, 2H), 5.50 (s, 1H), 6.85 (d, *J* = 8.7 Hz, 1H), 6.97 (d, *J* = 8.1 Hz, 1H), 7.06-7.08 (m, 1H), 7.17 (d, *J* = 7.8 Hz, 1H), 7.30 (s, 1H), 7.42-7.50 (m, 3H), 7.72 (d, *J* = 8.1 Hz, 1H), 8.19 (d, *J* = 7.2 Hz, 1H) ppm; ^{13}C NMR ($CDCl_3$, 100 MHz): *δ* 25.6, 25.8, 31.9, 38.1, 42.2, 51.5, 103.9, 124.7, 125.3, 126.6, 129.9, 130.5, 131.4, 132.1, 132.6, 133.6, 134.5, 137.7, 140.4, 145.9, 150.6, 209.9 ppm; IR (KBr): 1033, 1176, 1248, 1375, 1607, 2957, 3070 cm^{-1}; Mass (ES)$^+$ calcd. for $C_{26}H_{24}O_2$: 368.4; found m/z 391.1 [M + Na]$^+$]$^+$; Anal. calcd. for $C_{26}H_{24}O_2$: C, 84.75; H, 6.57 %; found: C, 83.99; H, 6.89 %.

12-(4-hydroxy-3-methoxyphenyl)-9,9-dimethyl-9,10-dihydro-8*H*-benzo[*α*]xanthen-11(12*H*)-one (4n) mp 164°C - 167°C; ^{1}H NMR ($CDCl_3$, 400 MHz): *δ* 1.08 (s, 3H), 1.18 (s, 3H), 2.20-2.23 (m, 1H), 2.27-2.29 (m, 1H), 2.62 (s, 2H), 3.58 (s, 3H), 4.75 (s, 1H), 5.38 (s, 1H), 6.38-6.50 (m, 1H), 6.52 (s, 1H), 6.55-6.65 (m, 2H), 6.70-6.78 (m, 1H), 7.28-7.53 (m, 2H), 7.75-7.80 (m, 1H), 8.08-8.1 (m, 1H), 8.18-8.24 (m, 1H) ppm; ^{13}C NMR ($CDCl_3$, 100 MHz): *δ* 27.5, 34.2, 37.6, 41.5, 50.8, 55.6, 114.0, 114.2, 121.6, 124.1, 124.4, 126.2, 126.4, 126.6, 127.5 ppm; IR (KBr): 762, 1033, 1147, 1228, 1271, 1374, 1430, 1512, 1622, 2958, 3064 cm^{-1}; Mass (ES+)calcd. for $C_{26}H_{24}O_4$ 400.4; found m/z 401.5 [M + H]$^+$]$^+$; Anal. calcd. for $C_{26}H_{24}O_4$: C, 77.98; H, 6.04 %; found: C, 77.83; H, 6.13 %.

12-(3,4-dihydroxyphenyl)-9,9-dimethyl-9,10-dihydro-8*H*-benzo[*α*]xanthen-11(12*H*)-one (4o) mp 137°C - 140°C; ^{1}H NMR ($CDCl_3$, 400 MHz): *δ* 1.05 (s, 3H), 1.09 (s, 3H), 2.18 (d, *J* = 16.4 Hz, 1H), 2.24 (d, *J* = 16.4 Hz, 1H), 2.63 (s, 2H), 4.89 (s, 1H), 6.58-6.64 (m, 5H), 7.11 (d, *J* = 8.4 Hz, 1H), 7.43 (d, *J* = 8.4 Hz, 1H), 7.49 (t, *J* = 7.6 Hz, 1H), 7.70 (t, *J* = 8.0 Hz, 1H), 8.17 (d, *J* = 8.4 Hz, 1H) ppm; ^{13}C NMR ($CDCl_3$, 100 MHz): *δ* 28.1, 31.2, 36.5, 40.4, 49.9, 112.6, 114.2, 114.3, 118.6, 122.6, 123.2, 125.2, 125.3, 126.1, 126.6, 131.9, 137.0, 142.3, 142.7, 143.5, 162.9, 196.0 ppm; IR (KBr): 760, 1057, 1180, 1232, 1372, 1466, 1519, 1613, 2962, 3466 cm^{-1}; Mass (ES+) calcd. for $C_{25}H_{22}O_4$ 386.4; found m/z 387.1 [M + H]$^+$]$^+$; Anal. calcd. for $C_{25}H_{22}O_4$: C, 77.70; H, 5.74 %; found: C, 77.65; H, 5.83 %.

4. CONCLUSION

In summary, we have established an alternative procedure for the three-component synthesis of benzo[*α*] xanthen-11-one derivatives using KF-Al_2O_3 as a recyclable catalyst. The prospect of the reusability of the catalyst has also been determined without compromising on the yield of the products.

Hence, the protocol presented here gives a simple alternative to many of the reported procedures by the use of KF-Al_2O_3 as an inexpensive, efficient and recyclable solid- support catalyst through simple workup procedure by simple filtration method.

Acknowledgement

The author thanks the SAIF, North-Eastern Hill University for the spectral analyses.

REFERENCES

[1] Hafez, H. N., Hegab, M. I., Ahmed-Farag, I. S.; El-Gazzar, A. B. (2008). A facile regioselective synthesis of novel *spiro*-thioxanthene and *spiro*-xanthene-9', 2-[1, 3, 4] thiadiazolederivatives as potential analgesic and anti-inflammatoryagents. *Bioorg. Med. Chem. Lett*. *18,* 4538.

[2] Lambert, R. W., Martin, J. A., Merrett, J. H., Parkes, K. E. B., Thomas, G. J. (1997). Preparation of pyrimidine nucleosides as thymidine kinase inhibitors and virucides. PCT Int. Appl. WO 9706178, *1997,* 79; *Chem*. *Abstr*. *126,* 21377y.

[3] Hideo, T., Teruomi, J. (1981). Benzopyrano [2, 3 - *b* xanthenesderivatives. *Jpn. Patent* 56, 005, 480, 1981. *Chem. Abstr*, *Vol. 95, 1981,* 80922b.

[4] Poupelin, J. P., Saint-Ruf, G., Foussard-Blanpin, O., Narcisse, G., Uchida-Ernouf, G., Lacroix, R. (1978). Synthesis and Antiinflammatory Properties of Bis(2-Hydroxy, 1-Naphthyl) Methane Derivatives. *Eur. J. Med. Chem*. *13,* 67-71.

[5] (a) Buu-Hoi, N. P., Saint-Ruf, G., De, A., Hieu, H. T. (1972). Inducing or inhibitory activity of dibenzo [*a*, *j*]-and dibenzo [*c*, *h*] xanthenes or zoxazolamine hydroxylase synthesis in vivo: Molecular structure-activity relations. *Bull. Chim. Ther*, 7, 83-6; (b) Saint-Ruf, G.; Hieu, H. T.; Poupelin, J. P. (1975). *Naturwissenschaften 62*, 584-585.

[6] (a) Ion, R. M., Planner, A., Wiktorowicz, K., Frackowiak, D. (1998). The incorporation of various porphyrins into blood cells measured via flow cytometry, absorption and emission spectroscopy. *Acta Biochim. Pol*. 45, 833-845; (b) Ion, R.M. (1997). The photodynamic therapy of cancer-a photosensitization or a photocatalytic process. *Prog. Catal*. *6,* 55-76.

[7] (a) Banerjee, A., Mukherjee, A. K. (1981). Chemical aspects of santalin as a histological stain. *Stain Technol*. 56, 83-85; (b) Menchen, S. M., Benson, S. C., Lam, J. Y. L., Zhen, W., Sun, D., Rosenblum, B. B., Khan, S. H., Taing, M. (2003). Sulfonated Diarylrhodaminede Dyes. *Chem. Abstr.*139, p54287f, U.S. Patent 6,583, 168, 2003.

[8] (a) Ahmad, M., King, T. A., Ko, D.-K., Cha, B. H., Lee, J. (2002). Performance and photostability of xanthene and pyrromethene laser dyes in sol-gel phases. *J. Phys. D*: *Appl. Phys*. 35, 1473-1476; (c) Knight, C. G., Stephens, T. (1989). Xanthene-dye-labelled phosphatidylethanolamines as probes of interfacial pH. Studies in phospholipid vesicles. *Biochem. J*. *258,* 683-687.

[9] (a) Kikuchi, K., Komatsu, K., Nagano, T. (2004). Zinc sensing for cellular application. *Curr. Opin. Chem. Biol*. 8, 182-191; (b) Knight, C. G., Stephens, T. (1989). Xanthene-dye-labelled phosphatidylethanolamines as probes of interfacial pH. Studies in phospholipid vesicles. *Biochem. J*. 258, 683-687*;* (c)

Buehler, C. A., Cooper, D. E., Scrudder, E. O. (1943). The stability of 2,2'-Dihydroxydiphenylmethane. *J. Org. Chem.8*, 316-319.

[10] Khurana, M. J., Magoo, D.(2009). pTSA-catalyzed one-pot synthesis of 12-aryl-8,9,10,12-tetrahydrobenzo[*a*] xanthen-11-ones in ionic liquid and neat conditions. *Tetrahedron Lett*. 50, 4777.

[11] Wang, H. J., Ren, X. Q, Zhang, Y. Y., Zhang,Z. H. (2009). Synthesis of 12-Aryl or 12- alkyl-8,9,10,12-tetrahydrobenzo[*a*]xanthen-11-one derivatives catalyzed by dodecatungstophosphoric acid. *J. Braz. Chem. Soc.* 20, 1939-1943.

[12] Nandi, G. C., Samai, S., Kumar, R., Singh, M. S. (2009). An efficient one-pot-synthesis of tetrahydrobenzo[*a*]xanthene-11-one and diazabenzo[*a*]anthracene-9,11-dione derivatives under solvent free conditions.*Tetrahedron 65,* 7129-7134.

[13] Li, J., Li, Y-W., Song, Y-L. (2012). Efficient synthesis of 12-aryl-8, 9, 10, 12- tetrahydrobenzo[*a*]xanthen-11-one Derivatives catalyzed byp-dodecylbenzenesulfonic acid in aqueous media under ultrasound irradiation. *Synth. Commun.* 42, 2161-2170.

[14] Karimi, N., Oskooie, H. A., Heravi, M. M., Tahershamsi, L. (2010). Caro's acid-Silica Gel-Catalysed One-Pot Synthesis of 12-Aryl-8,9,10,12 tetrahydrobenzo*[a]* Xanthen-11-ones.*Synth. Commun*. *41*, 307-312.

[15] Sethukumar, A., Vithya, V., Kumar, C. U., Prakasam, B. A. (2012). NMR spectral and structural studies on some xanthenones and their thiosemicarbazone derivatives: Crystal and molecular structure of 12-(2-chlorophenyl)- 8, 9, 10, 12-tetrahydrobenzo[*a*]xanthen-11-one. *J. Mol. Struct.* 1008, 8-16.

[16] Mo, L-P., Chen H-L. (2010). One-pot, Three-component Condensation of Aldehydes, 2-Naphthol and 1,3-Dicarbonyl Compounds. *J. Chin. Chem. Soc*. *57*, 157-161.

[17] Foroughifar, N., Mobinikhaledi, A., Moghanian, H., Mozafari, R., Esfahani, H. R. M. (2011). Ammonium chloride catalyzed one-pot synthesis of tetrahydrobenzo[*a*]xanthen-11-one derivatives under solvent-free conditions. *Synth. Commun. 41*, 2663-2673.

[18] Oskooie, H. A., Heravi, M. M., Karimi, N., Kohansal, G. (2011). Cu/SiO_2-Catalyzed One-Pot Synthesis of 12-Aryl-8,9,10,12-tetrahydrobenzo[*α*] xanthen-11-ones Under Solvent-Free Conditions. *Synth. Commun*. *41*, 2763-2768.

[19] Wang, R-Z., Zhang, L-F., Cui, Z-S. (2009). Iodine-Catalyzed Syynthesis of 12-Aryl-8,9,10,12-tetrahydrobenzo[*a*] xanthen-11-one Derivatives *via* Multicomponent Reaction. *Synth. Commun*. *39*, 2101-2107.

[20] Nemati, F., Arghan, M., Amoozadeh, A. (2012). Efficient, Solvent-Free Method for the One-Pot Condensation of *β*-Naphthol, Aromatic Aldehydes, and Cyclic 1,3-Dicarbonyl Compounds Catalyzed by Silica Sulfuric Acid. *Synth. Commun*. *42*, 33-39.

[21] Kaur, B., Parmar, A., Kumar, H. (2012).

Manganese Perchlorate–Catalyzed Greener Synthesis of 12-Aryl or 12-Alkyl- 8, 9, 10, 12-tetrahydrobenzo[*α*] xanthen-11-one Derivatives Under Ultrasonication.*Synth. Commun*. *42*, 447-453.

[22] Zhang, Z-H., Zhang, P., Yang, S-H., Wang, H-J., Deng, J. (2010). Multicomponent, solvent-free synthesis of 12-aryl- 8, 9, 10, 12-tetrahydrobenzo[*a*]-xanthen-11-one derivatives catalysed by cyanuric chloride. *J. Chem. Sci*. *122*, 427-432.

[23] Rama, V., Kanagaraj, K., Pitchumani, K. (2012). A multicomponent, solvent-free, one-pot synthesis of benzoxanthenones catalyzed by HY zeolite: their anti-microbial and cell imaging studies. *Tetrahedron Lett*. *53*, 1018-1024.

[24] Fatma, S., Singh P. K., Ankit, P., Shireen, Singh, M., Singh, J. (2013). Thiamine hydrochloride as a promoter for the efficient and green synthesis of 12-aryl-8, 9, 10, 12-tetrahydrobenzoxanthene-11-one derivatives in aqueous micellar medium.*Tetrahedron Lett*. *54*, 6732-6736.

[25] Akondi, A. M., Kantam, M. L., Trivedi, R., Sreedhar, B., Buddana, S. K., Prakasham, R. S., Bhargava, S. (2014). Formation of benzoxanthenones and benzochromenones *via* cerium-impregnated-MCM-41 catalyzed, solvent-free, three-component reaction and their biological evaluation as anti-microbial agents. *J. Mol. Cat. A*: *Chemical* 386, 49–60.

[26] Olyaei, A., Alidoust, M. G. (2015). Rapid and Efficient One-Pot Green Synthesis of 12-Aryl- 8, 9, 10, 12-tetrahydrobenzo[*a*]xanthene-11-ones Using Zr-MCM-41 Catalyst. *Synth. Commun*., *45*, 94-104.

[27] Sadeghpour, M., Olyaei, A., Rezaei, M. (2016). Guanidine Hydrochloride: A Highly Efficient Organocatalyst for the Synthesis of 12-Aryl- 8, 9, 10, 12-tetrahydrobenzo[*a*]xanthene-11-ones Under Solvent-Free Conditions. *J. Heterocycl. Chem*. *53*, 981.

[28] Terra, B. S., Osorio, A. M. B., Oliveira, A. de., Santos, R. P.M., Mouro, A. P., Araújo, N. F. de., Silva, C. C. da.,Martins, F. T., Vieira, L. B., Bonaventura, D., Abreu, H. A. de., Alcântara, A. F. C., Fátima, A. de.,(2017). Natural Organic Acid as Green Catalyst for Xanthenones Synthesis: Methodology, Mechanism and Calcium Channel Blocking Activity. *J. Braz. Chem. Soc*. *28*, 2313-2325.

[29] Brahmachari, G., Nurjamal, K., Begam, S., Mandal, M., Nayek, N., Karmakar, I., Mandal, B. (2019). Alum ($KAl(SO_4)_2.12H_2O$) - An Eco-friendly and Versatile Acid-catalyst in Organic Transformations: A Recent Update. *Current Green Chemistry*. *6*, 12-31.

[30] (a) Abramovitch, R. A. (1991). Applications of Microwave Energy in Organic Chemistry. A Review. *Org. Prep. Proc. Int*. *23*, 683-711; (b) Bose, A. K., Manhas, M. S., Ghosh, M., Raju, V. S., Tabei, K., Urbanczyk-Lipkowska, Z. (1990). Highly accelerated reactions in a microwave oven: synthesis of heterocycles. *Heterocycles 30*, 741-744;(c) Villemin, D., Ben Alloum, A. (1993). Potassium Fluoride on Alumina: Con-

densation of 3-methyl-2-thiono-4-thiazolidinone with aldehydes Synthesis of *α*-thioacrylic acids and phosphonothionothi azolidinones. *Phosph. Sulf. Silic*. *79*, 33-41; (d) Puciová, M., Ertl, P., Toma, S. (1994). Synthesis of Ferrocenyl-Substituted Heterocycles: The Beneficial Effect of the Microwave Irradiation. *Collect. Czech Chem. Commun*. *59*, 175-185; (e) Lácová, M., Chovancová, J., Veverková, E., Toma, S. (1996). Microwaves assisted Gabriel synthesis of phthalides. *Tetrahedron 52*, 14995-15006.

[31] Lidström, P., Tierney, J., Wathey, B., Westman, J. (2001). Microwave assisted organic synthesis - a review. *Tetrahedron 57*, 9225-9283.

[32] Kharbangar, I., Rohman, Md. R., Mecadon, H., Myrboh, B. (2012). KF-Al_2O_3 as an Efficient and Recyclable Basic Catalyst for the Synthesis of 4*H*-Pyran-3-carboxylates and 5-Acetyl-4*H*-pyrans.*Int. J. Org. Chem.2*, 282-286.

Research article:

photosav: A Tkinter Based Photo Editing Application

Rahul Kumar Singh[1], Deepjyoti Choudhury[1*] and Arpita Sen[2]

[1]Techno India University, Kolkata, West Bengal, India
[2]Manipal University, Jaipur, Rajasthan, India

Article Info:
https://doi.org/10.54290/spect/2022.v9.1.0003

Received: August 29th, 2022
Revised: October 25th, 2022
Accepted: October 30th, 2022

Corresponding author:
deepjyotichoudhury05@gmail.com

Abstract: The human brain is more engaged by viewing images than by reading lists of facts. Whenever we try to view, edit, or create an image, we actually have our own intera tion with the visual expression in the image. Although ever one has a unique editing style, it is a common practice in the photography industry. Photo editing enable users to enhance and stylize images in ways that would be impossible in camera. It is much more difficult without image editing application. This paper presents an approach for the development of Windows application that can be a full-scale photoe diting tool. Our application is easy to use and it also helps to store images via different extensions. The various image editing libraries used to develop this application are explained here. Different image editing features such as cropping, drawing, etc. help all type of users to use the application efficiently. The detailed explanation of these features are provided. This paper shows how image processing can be used to edit images by using various computer vision algorithms to perform several operations on an image. However, there are certain image editing applications available, but photosav is a simple and comprehensive windows application in which maximum features are clubbed together for the users.

Keywords: *Tkinter, computer vision, GUI, image, windows application.*

1. INTRODUCTION

An image is a matrix of pixels. When we see an image on screen, it is nothing but small boxes called pixels of different brightness that help in forming an image. Thus, for a viewer, images can be seen in different formats. For example, VGA, HD, etc [1]. Today, in our day-today life, we click various images using our mobile phones. Photos are further enhanced and corrected for artistic rea-

How to Cite:
Shing et al.(2022). photosav: A Tkinter Based Photo Editing Application. *Spectrum: Science and Technology, v9 (1), 25-33.* https://doi.org/10.54290/spect/2022.v9.1.0003

sons. Now, in order to edit a particular image, an ideal image editing tool will be able to give the user a choice to change the image according to their preference [2, 3, 4]. It is actually not possible because we cannot read the user's mind and synchronise with the required image entities the users want. We can take the help of computer vision algorithm to construct and make it available for the users. There are many image editing applications, for example Photoshop [5, 6], which has comprehensive features for editing images. There are several other applications for specific purposes of photo editing, for example, Luminar. Many image processing tasks, including image editing, have benefited from multi-scale image decompositions such as the Laplacian pyramid [7]. The ability to modify the 'appearance' and 'fine details' of the image is a practical advantage of considering multiple scales for image editing [9, 8]. On the downside, the results obtained from enhancing fine details in the well known halo artefacts are considered as unnatural images.

This paper aims to present the methods for creating an easy- to-use image editing application that can edit the image as well as save the image in different formats. phototsav has been developed to serve this purpose. This paper shows the complete procedure of the development of the editing application from scratch. The application provides a detailed way to edit images with a wide variety of digital image processing techniques incorporated with a graphical user interface. The result is given with a step-by-step demonstration to edit a photo and get the desired result at the end.

There are four sections elaborated in the paper. Following the introduction in the first section, the second section explains the techniques, methods, and software solutions used in the application development process. The third section shows how applications can be used to edit images, either to improve image quality or to achieve certain artistic effects. The final section presents the conclusion and emphasises the benefits and utility of this application.

2. DESIGN AND IMPLEMENTATION

2.1. Framework and language

Tables The photosav is developed using Tkinter [10, 9] which is a Python library to create Graphical User Interfaces (GUIs). The programming language framework used for development is OpenCV-Python [10] which is a Python wrapper for the original OpenCV C++ implementation. Different other packages are used, including numPy [11], filedialog, etc. OpenCV is used for the inbuilt image processing functions and algorithms that make image editing easier.

2.2. Photosav functionalities

During image editing the various changes should be seen on screen simultaneously. To do that, we have created a canvas [9] using Python where we can display our edited or filtered image. The user makes certain changes to the image. Those changes are seen side by side on the screen. The main purpose of photosav is to help users to have a custom experience while using the application. Since photosav is a single-page application, the users will find all the features in one place. As soon as the image is ed-

ited, the user can apply the changes or revert to the original image, and then save the image in any format supported by openCV [10] such as png, tiff, jpeg, etc. photosav has several features to give the best user experience, such as cropping, drawing, adding text, negative action, black and white action, stylisation, sketch effect, embosses, sepia, binary thresholding, erosion, dilation, flipping the image, rotation of the image, blurring and smoothing, adjusting brightness and saturation.

2.3. Image Processing Techniques

This section will elaborate most of the image editing functionalities used in photosav. Here, many features such as brightness and saturation take user inputs using the GUI. So the results are mostly custom and vary from user to user. Some of the well known methods such as rotation, flip or Gaussian blur are Also used in the development of the phototsav.

2.3.1 Contrast and Brightness Method

These functions control the pixel matrix. If we want to increase the brightness of an image, we have to add a positive constant value to each and every pixel in the image i.e., o(i,j) = o(i,j) +a, where i and j are the row and column of the pixel matrix and a is the constant.

A simple way to control the contrast and brightness using the function is

$$p(x) = \alpha.f(x) + \beta p(x) \quad (1)$$

here β is the brightness and coefficient α is contrast

2.3.2 Cropping, Drawing and Adding text functions

In open CV algorithms, there is no predefined formula for cropping, sketching, or adding text to an image. The NumPy array slicing technique facilitates our work. A 2D array is used to store each image pixel matrix that is read (for each colour channel). We can simply define the region to be cropped in height and breadth (in pixels). We can use the numPy array to choose a specific area, add text, and draw on the image.

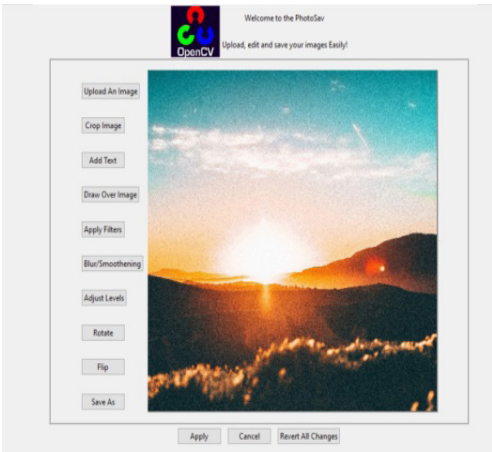

Cropping functionality: To crop an image, we have to resize the pixel matrix, which can be easily done by the "resize" function in openCV. When we perform this operation by using the GUI, by using three events (click, drag, and release). Firstly, we can draw a rectangle using the coordinates (starting and ending) and the region of focus is passed to OpenCV. As mentioned, there are three events (button pressed, button in motion, and button released), we will record the starting coordinates from the first event. When the value of the coordinates are zero, while we are in motion,

many points are generated, but we will consider the latest points and save the ending points. Now we can easily create a rectangle using the canvas "create rectangle" function (in this function, we can pass all the four coordinates). The rectangle will be clearly visible on the canvas. Now we need to remove the rectangle and pass the four values to the slice object and, with the help of openCV, the images are cropped. There are many ways to crop an image. We can start from any point, so we have to record the starting and ending of the rectangle and pass them properly.

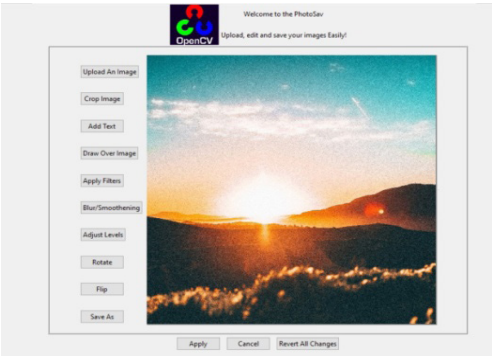

(a) Original Image

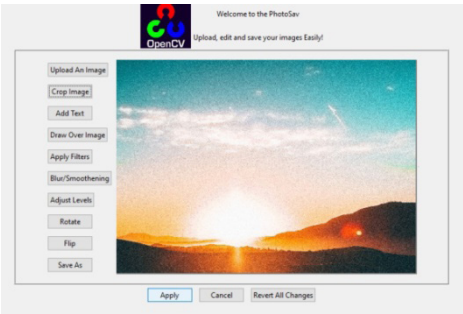

(b) Edited Image

Figure 1. Cropping using photosav

Drawing functionality – When the draw button is clicked, openCV takes the inputs for two events (button pressed and button in motion). We have a default color frame, a color chooser from the color palette which enables the user to use color from the color palette. The function will return a hexadecimal value, when the button is pressed. The "start draw" function is called and while the button is in motion, "start draw" expect an event (x and y) exactly when the button is clicked. We can maintain the values in a list and update the list when the the point is dragged. The time we draw on canvas to create small lines, the starting and ending coordinates are provided based on four coordinates using openCV. We have to append the four coordinates with new values because one line is needed to be connected to the first line and every time the line ends, a new line starts until the button is dragged and then stopped. To show this on canvas we can use "cv2.line" function [10], where we will pass the filtered image, all the four updated coordinates, color and thickness of the line (vary with the size of the image).

Adding text- When we click on the "adding text" button, we have two options, enter the text and choose the colour. These are identical to the cropping process except that instead of cropping here, we have to place the text on the image. In this process, we will also use the click, drag and release events. The rectangle is first created by using the coordinates and canvas. "Create rectangle" function is called to form the rectangle and while it is deleted, release event is called. Basically, we will consider the text and color of the text as an input. In this function, we have to pass the image, the text, the color, and a function in tkinter named "puttext" that helps to write on the image, the thickness and

the color code. Here, we have to convert the BGR format to RGB format as opencv support BGR format. Moreover we will display the image on the canvas using the "display image" function.

2.4. Filter function

There are certain filter functions in photosav for the user to change the original image.

2.4.1 Bitwise operation

There are various bitwise operations which we can perform on the original image to get a new image such as Bitwise NOT. Bitwise NOT turn the pixel value in the pixel matrix. All the pixel values that are greater than zero are set to zero, whereas all pixels that are equal to zero are set to 255 [10]. Thus we can see the image in black and white.

2.4.2 Stylization action

It is considered to create a cartoonized / stylized image with the help of openCV function Stylization [10] . The result of stylization function looks like a painted image.

2.4.3 Sepia action

Sepia toning is the process of coloring a photograph with a brownish color to give it an aesthetic or vintage appearance. Sepia action [12] is performed as a linear transformation of each pixel value with a linear operator, using each pixel of an image as an array [B G R] T, where B, G, and R represent the blue, green, and red components of an RGB color space. The equation. 2 explains the Kernel matrix value as shown in below:

$$S^{sepia} = \begin{bmatrix} 0.272 & 0.534 & 0.131 \\ 0.349 & 0.686 & 0.168 \\ 0.393 & 0.769 & 0.189 \end{bmatrix} (2)$$

It is simple to implement in OpenCV. It has a defined colour. It includes a standardised matrix that can be set to be the default. OpenCV implements the BGR colour format, whereas the matrix in equation. 2 uses the RGB colorspace. Therefore, it has to be converted to RGB, then back to BGR after processing before displaying the output image on the canvas.

2.4.4 Erosion and dialation

Erosion usually includes eroding the outer surface of the image. Because binary images only have two pixels (0 and 255), it primarily involves eroding the image's foreground, which should be white. The depth of erosion is determined by the size and shape of the defined kernel. To define a kernel, we can use NumPy's ones() function. Other functions, such as NumPy zeros, customised kernels, and others, can be used to define kernels based on the problem.The binary equation to perform erosion is:

$$dst(x, y) = \min_{(x', y')} : element(x', y')^{=0^{src(x+x', y+y')}} \quad (3)$$

Dilation entails distorting the outer surface of the image. It is the polar opposite of the erosion operation. The dilation operation is convolving an image P with some kernel B of any shape or size. The kernel Q has a defined anchor point, which itself is usually the kernel's centre. We compute the maximum pixel value overlapped by Q as the kernel Q is scanned over the image and substitute the image pixel in the anchor point position with that maximal

value. As one might expect, this maximizing operation causes bright parts of the image to shine. The binary operation to perform dilatation is:

$$dst(x,y) = max_{(x',y'):element(x',y')=0} src(x+x', y+y') \quad (4)$$

2.5. Graphical user Interface

photosav can run on any computer with windows as an operating system. When we run the application the user can import an image using "upload" button and that image can be seen on the canvas. All the tools present in the application are easy to use. After uploading the image user can perform various editing operation from the main menu (Figure. 2(a)). Moreover, most of the operations will appear on the additional side menu which have sliders. To add text on the image, the users have to choose the color of text [9] using color chooser which will popup on screen. After using a certain tool, users can see the change on screen simultaneously. User can click on "apply" button to apply the changes or even click "cancel" button if the edit is not satisfactory. After applying changes if the user want to see the original image user can click on "revert" button to reverse the changes and then the original image will appear. To enable working with various size of the image, very large image automatically rescale to fit in photosav.

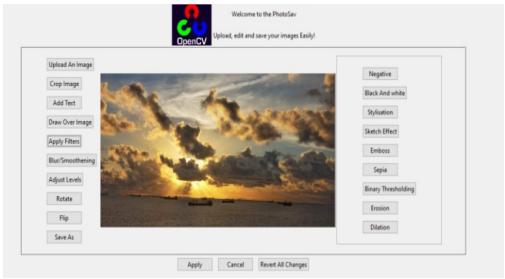

(a)

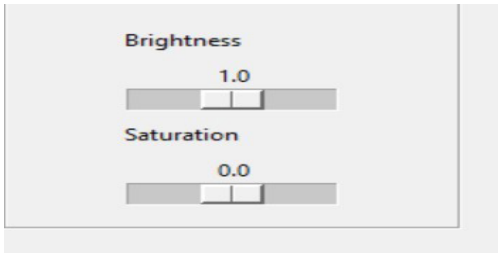

(b)

Figure 2. Graphical user interface

3. RESULTS AND DISCUSSION

The various image editing functions such as rotation, flip, cropping, adding text, etc. can be combined with other functions in photosav will give a custom change in the edited image. If the user does not like a certain feature, then the user can revert the changes accordingly. It provides the confidence to the user to edit the image without losing the previous change

3.1. Results of photo editing

Figure. 3 explains the step by step procedure of editing an image in photosav. To edit the image we take an input image (Figure. 3(a)). At first, we apply erode as well as dilute function on the image to remove the noise. Next we apply stylization function to give an cartoonistic appearance to the image. Then, we use the horizontal flip action and at last we use black and white action to change the final result (Figure. 3(f)).

(a) original (b) erode

(c) dilute (d) stylization

(e) horizontal flip (f) black and white

Figure 3. Image edited using photosav

3.1. Different editing example

Figure. 4(b), Figure. 5(b), Figure. 6(b) Figure. 7(b), Figure. 8(b), Figure. 9(b) and Figure. 10(b) are the edited images with different filtering/editing tool used in the photosav application. Figure. 4(a) is an input image edited using Black and white feature followed by adding text "Hello". Figure. 5(a) is edited by adjusting the saturation value to 29.5 and brightness value to 1.4. On Figure. 6(a) we have applied rotate left feature and black and white feature. Figure. 7(a) is flipped vertically by the flip function and then we have applied negative function. Figure. 8(a) is edited by adjusting the saturation and brightness value. The input image Figure. 9(a) is enhanced using stylization function followed by blurring the image then adjusting the saturation value to -12.0 lastly eroding and diluting the image. Last but not the least Figure. 10(a) corrected by adjusting the blur function followed by diluting and eroding the image.

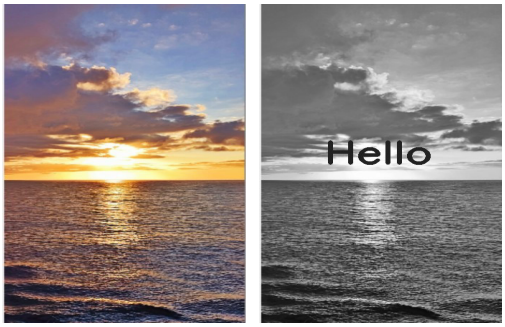

(a) Original image (b) Edited Image

Figure 4. Image edited using adding text "Hello" and Black and white feature.

(a) Original image (b) Edited Image

Figure 5. Image edited by adjusting the saturation and brightness value

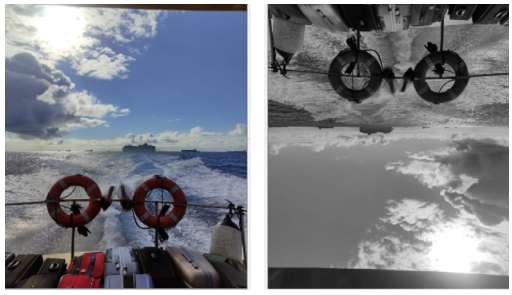

(a) Original image (b) Edited Image

Figure 6. Image edited by user using rotate left and black and white feature.

(a) Original Image

(b) Edited image

Figure 7. Image edited by flipping the image vertically and then applying negative function.

(a) Original image (b) Edited Image

Figure 8. Image edited by adjusting the saturation and brightness value.

(a) Original Image

(b) Edited Image

Figure 9. Image edited using stylization function followed by blurring the image then adjusting the saturation values then eroding and diluting the image.

(a) Original Image

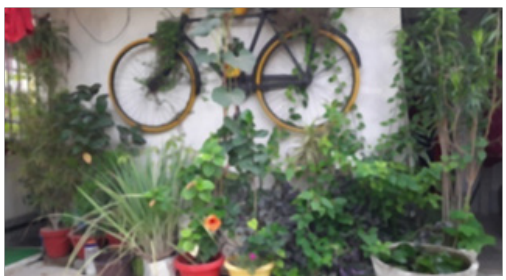

b) Edited image

Figure 10. Image edited by adjusting the blur function followed by diluting and eroding.

3. CONCLUSION

photosav provides users with basic photo to editing functions and allows them to complete a wide range of tasks. It is suit-

able from moderate to complex photo corrections and excels at brightness and contrast manipulation. Furthermore, when using editing tools, it revitalises the user's imagination. Color adjustment, focusing, effects, geometric transformations, saturation, hue, colour map, and brightness changes are all available in this application. It allows the users to express their creativity and imagination. The tools are useful for creating imaginative, abstract, and stylized images in which colours and shapes behave differently than they do in reality.

In future photosav could be improved by adding more photo manipulation tools as well as more Image enhancement features. It may also include the redesign and enhancement of existing tools.

REFERENCES

[1] Saund, E., & Moran, T. P. (1994). A perceptually-supported sketch editor. In *Proceedings of the 7th annual ACM symposium on User interface software and technology* (175-184).

[2] Saund, E., Fleet, D., Larner, D., & Mahoney, J. (2003). Perceptually-supported image editing of text and graphics. In *Proceedings of the 16th annual ACM symposium on User interface software and technology* (183-192).

[3] Saund, E. (2003). Finding perceptually closed paths in sketches and drawings. *IEEE transactions on pattern analysis and machine intelligence*, *25*(4), 475-491.

[4] Cao, Q. R., Choi, H. G., Kim, D. C., & Lee, B. J. (2004). Release behavior and photo-image of nifedipine tablet coated with high viscosity grade hydroxypropylmethylcellulose: effect of coating conditions. *International journal of pharmaceutics*, *274*(1-2), 107-117.

[5] Lehr, H. A., Mankoff, D. A., Corwin, D., Santeusanio, G., & Gown, A. M. (1997). Application of photoshop-based image analysis to quantification of hormone receptor expression in breast cancer. *Journal of Histochemistry & Cytochemistry*, *45*(11), 1559-1565.

[6] Yadav, S. (2022). Photoshop: Create image blur: It's all a blur. *Australian Photography*, 44-51.

[7] Burt, P. J. (1983). EH Adelson The Laplacian Pyramid as a compact image code. *IEEE Transactions on Communications*, *31*(4), 532-540.

[8] Li, Y., Sharan, L., & Adelson, E. H. (2005). Compressing and companding high dynamic range images with subband architectures. *ACM transactions on graphics (TOG)*, *24*(3), 836-844.

[9] Grayson, J. E. (2000). *Python and Tkinter programming*. Manning Publications Co. Greenwich.

[10] Howse, J. (2013). *OpenCV computer vision with python*. Birmingham: Packt Publishing.

[11] Oliphant, T. E. (2006). *A guide to NumPy* (Vol. 1, p. 85). USA: Trelgol Publishing.

[12] Komazec, T., & Gavrovska, A. (2020, November). Photo matching using skin color histogram without and with Instagram-like modifications. In *2020 28th Telecommunications Forum (TELFOR)* (pp. 1-4) . IEEE.

Research article:

Caffeine Extraction from Local Tea Leaves and its Estimation by Iodometric Method

Siewdorlang Diamai[1]*, Icydora Kharkongor[1], Eveningstar Ryntathiang[1] and Rodridge Russel Kharbudon[1]

Department of Chemistry, St Anthony's College, Shillong, Meghalaya, India

Article Info:
https://doi.org/10.54290/spect/2022.v9.1.0004

Received: October 4th, 2022
Revised: October 20th, 2022
Accepted: October, 30th, 2022

Corresponding author:
sdiamai@anthonys.ac.in.

Abstract: The principal constituent of tea, which is responsible for all the properties, is the alkaloid caffeine. Theanine is an amino acid found only in tea leaves, which imparts a pleasantly sweet taste to tea. It is degraded to glutamic acid and has relaxation effects in humans. Caffeine is a bitter, white crystalline xanthine alkaloid and a stimulant drug. It is found in varying quantities in the seeds, leaves, and fruit of some plants, where it acts as a natural pesticide that paralyses and kills certain insects feeding on the plants, as well as enhancing the reward memory of pollinators. It is also found in coffee, tea, cola, guarana, mate, and other products. Caffeine - containing products have been consumed for hundreds of years for their pleasant flavour and stimulating effects. Caffeine is one of the most commonly used stimulants among athletes. In this paper we have discuss the extraction of caffeine from our local tea leaves, *Namar Jongphi* and *Nalari Gold* tea leaves available in the market. The liquid-liquid extraction method was followed for the extraction of caffeine and the estimation of the amount of caffeine was calculated and estimated by iodometric method.

Keywords: Caffeine; *Namar Jongphi*; *Nalari Gold* Tea leaves; liquid-liquid extraction; iodometric method

1. INTRODUCTION

Caffeine comes from the German word "kaffee". Caffeine was first discovered by Friedlieb Ferdinand Runge. Since its discovery, caffeine is one of the most popular and widely consumed beverages in the world [1]. Caffeine belongs to a class of purine alkaloids and its main source is coffee. However, other sources

How to Cite:
Diamai et al.(2022). Caffeine Extraction from Local Tea Leaves and its Estimation by Iodometric Method. *Spectrum: Science and Technology, v9 (1), 35-41.* https://doi.org/10.54290/spect/2022.v9.1.0004

of caffeine can be obtained from leaves, fruits and seeds of many plants such as tea leaves, cola nuts, guarana berries, and cacao beans. It is worth pointing out that caffeine may also be found in energy drinks, soft drinks, gums, and medications [2,3]. Caffeine is bitter in taste. Chemically caffeine is named as 1,3,7-trimethyl-2,3,6,7-tetrahydro-1*H*-purine-2,6-dione and its molecular formula is $C_8H_{10}N_4O_2$ (Figure 1).

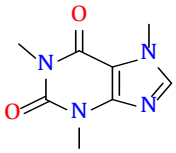

Figure 1. Structure of Caffeine

It has a molecular mass of 194.19 g/mol, melting point of 238 °C and is slightly soluble in water but the solubility increases as the temperature is increased. Recently, caffeine has been of scientific interest because, as a bioactive molecule, [1] it has been shown to have beneficial health effects (e.g., it is able to protect against oxidative stress in Alzheimer's disease (AD)) [4]. However, people with hypertension, children, adolescents, and the elderly may be more susceptible to the negative effects of caffeine consumption [5].

Tea is also one of the common beverages which are being enjoyed by many for its bitter, cooling and astringent flavour. Tea is obtained from the leaves of the tea plant, *Camellia sinensis*. The caffeine content of tea leaves depends on the variety and where they were grown; most tea has 3-5% by weight [9]. Based on our literature survey, liquid-liquid extraction is one of the most common methods of extraction of caffeine from tea [6-9]. Herein, we present our work on extraction of caffeine from tea by using two local tea brands N*amar Jongphi* (*NJP*) and *Nalari Gold* (*NLR)* tea. The caffeine was extracted by liquid-liquid extraction method and the amount of caffeine was estimated by iodometric method.

2. MATERIALS AND METHODS

2.1 *Materials*

The samples for study were purchased from the market. The two local tea brands NJP and NLR tea leaves were chosen for caffeine extractions and its estimation. We have followed the dichloromethane-water extraction method [6,9] for the extraction of caffeine from these two tea brands (Figure 2 and 3).

Figure 2: *Namar Jongphi t*ea leaves (*NJP*)

Figure 3: *Nalari Gold* tea leaves (*NLR*)

2.2 *Extraction of caffeine with dichloromethane*

Caffeine can be extracted from tea using the method known as liquid-liquid extraction (LLE). In this method, compounds are separated according to their

relative solubilities in two immiscible liquids, usually water and another organic solvent. In the extraction of caffeine from tea leaves the two liquids used are water and dichloromethane (DCM). Dichloromethane is chosen as the organic solvent because the percentage solubility of caffeine is quite high in DCM [10].

2.3 Procedure for extraction of caffeine:

In the first part of the experiment, 10 g of tea leaves is weighed and transferred to a 500 mL beaker. 6 g of sodium carbonate and 300 mL of distilled water are added to the beaker and the contents are boiled for about 15-20 minutes. Sodium carbonate is added to act as a base so it can react with the tannins to form their soluble sodium salts. After boiling, the mixture is allowed to cool and is filtered. The tea leaves are washed with water 3-4 times to wash away the caffeine stuck in the filter paper into the filtrate. The filtrate is then used for liquid-liquid extraction of caffeine. Caffeine is extracted by the use of a separating funnel. Vigorous shaking is not recommended since it leads to the formation of an emulsion which is difficult to separate. Dichloromethane is used as the organic solvent since caffeine is more soluble in it in comparison to other organic solvents. The tannins in their sodium salt forms are ionic in nature and hence are insoluble in dichloromethane but soluble in water.

The solution of caffeine in dichloromethane is collected and is mixed with anhydrous sodium sulphate to absorb any water that might have been in the solution of caffeine. The anhydrous solution of caffeine in dichloromethane is then transferred into a round bottom flask and the solution is then distilled using a water bath to obtain crude caffeine. The crude caffeine thus obtained was purified by sublimation. The melting point of the purified caffeine was measured using a capillary melting point apparatus and the melting point was found to be 237-238 ^{o}C and analysed using IR spectroscopy and the amount estimated by Iodometry Back Titration.

2.4 Iodometric estimation of caffeine:

There are several analytical methods for the estimation of caffeine [11]. In our experimental work, we have used the iodometric back titration for the estimation of the amount of caffeine extracted from the two varieties of tea leaves. In Iodometric Back Titration, caffeine reacts with excess accurately known amount of iodine in acidic environment, forming insoluble precipitate. Then the insoluble precipitate is removed by filtration. Using titration by a standard sodium thiosulphate solution (Scheme 1) with starch solution as indicator, we can determine the amount of remaining iodine, and thus the amount of caffeine can be found [11].

Scheme 1

3. RESULTS AND DISCUSSION

3.1 IR spectroscopy

IR spectroscopy is an analysis technique where an organic chemist can readily examine the common functional groups of organic compounds. Functional groups in organic compounds have absorptions which are characteristics not only in position but also in intensity [12]. Thus, the purified caffeine that was obtained was analysed by IR spectroscopy to identify the important functional groups (C=O, C=N, C-N, C-H) (Figure 4).

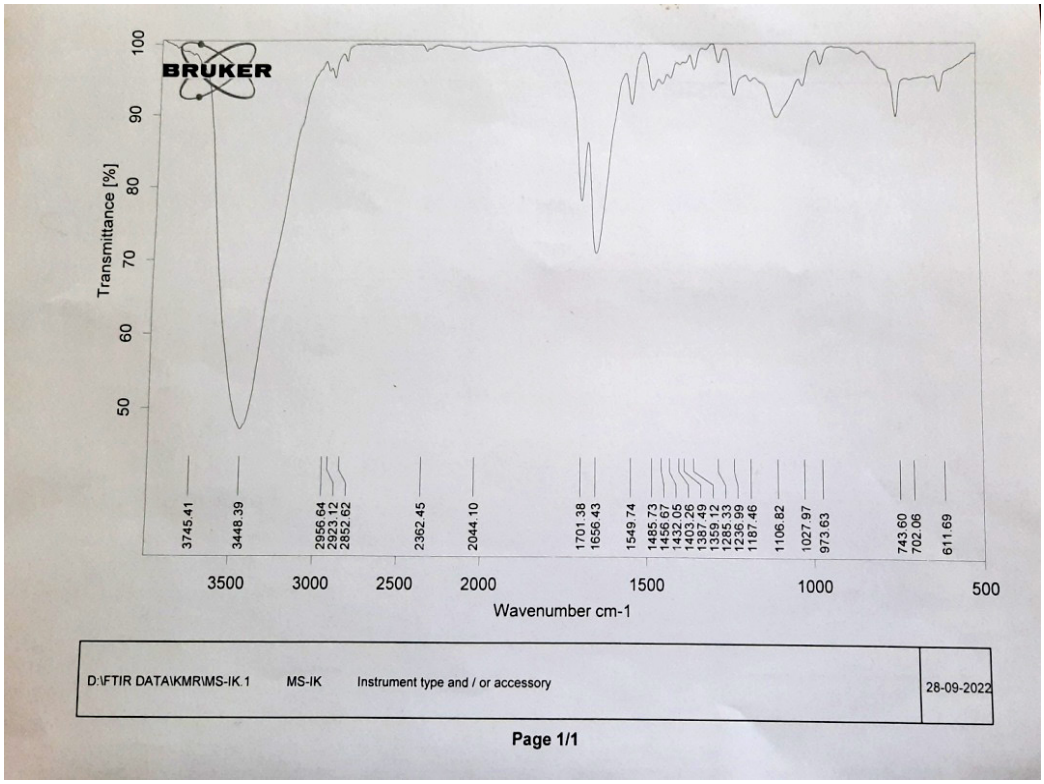

Figure 4: IR spectrum of caffeine

3.2 Estimation of caffeine by Iodometric back titration

Caffeine solution was prepared using 0.05 mol/L sulphuric acid as an acidic medium. Stock solution of NJP was prepared by dissolving 0.347 g in 50ml and NLR by dissolving 0.224 g in 50 ml. 0.05 mol/L iodine solution was added to the caffeine content. A reddish-brown precipitate is formed after the addition of iodine solution (Figure 5). Then the insoluble precipitate is removed by filtration. The filtrate containing the excess iodine was titrated against sodium thiosulphate of strength 0.05 mol/0.005 mol till the solution becomes pale brown in colour.

Figure 5: Formation of insoluble precipitate

Then starch was added as indicator after the solution becomes dark brown. Upon the addition of starch indicator, a dark brown solution is obtained which when titrated with sodium thiosulphate whereby the solution changes to dark blue, with further titration the colour of the solution turns colourless which marks the end point of the reaction. The volume of thiosulphate consumed is equivalent to the amount of unreacted iodine present in the solution and hence the amount of caffeine was calculated [11].

Table 1: Iodometric titration for caffeine extracted from *Namar Jongphi* tea leaves

(Amount extracted from 10 grams of NJP is 0.347g)

Sl. no	**Sample** Namar Jong phi (mL) (0.03474 mol)	Volume of H_2SO_4 (mL) (0.05 mol)	Volume of I_2 (mL) (0.05 mol)	Volume of $Na_2S_2O_3$ (mL) (0.05 mol)
1	10	10	10	1.3
2	10	10	10	1.3
3	10	10	10	1.2
4	10	10	10	1.1

Calculations:

Amount of crude caffeine extracted (NJP) and taken for estimation = 0.347g

Concentration of caffeine = 0.03574 mol (0.347g in 50 mL)

Volume of caffeine taken for titration = 10 mL

Volume of I_2 added = 10 mL

No. of moles of I_2 added = (10 ÷ 1000) × 0.05 mol = 5×10^{-4} mol ---------- (i)

No. of moles of $Na_2S_2O_3$ = (1.3 ÷ 1000) × 0.05 mol = 6.5×10^{-5} mol

From the equation:

$$I_2 + 2Na_2S_2O_3 \longrightarrow 2NaI + Na_2S_4O_6$$

Number of moles of I_2 reacted with $Na_2S_2O_3$ (excess I_2) = 6.5×10^{-5} mol/2 = 3.25×10^{-5} mol

Therefore, number of moles of I_2 reacted with caffeine = (total iodine added – excess iodine)

= 5×10^{-4} mol - 3.25×10^{-5} mol = 4.675×10^{-4} mol

From the equation:

$$C_8H_{10}N_4O_2 + 2I_2 + KI + H_2SO_4 \longrightarrow C_8H_{10}N_4O_2.HI.I_4 + KHSO_4$$

Number of moles of caffeine reacted with iodine = 4.675×10^{-4} mol/2 = 2.3375×10^{-4} mol

Therefore, amount of caffeine in 10 mL = 2.3375×10^{-4} mol ×194.19 g/mol = 0.04539 g

Thus, amount of caffeine in 50 mL = 0.04539×5 = 0.22695g

Amount of crude caffeine take (*Namar Jongphi*) = 0.347 g

Amount of caffeine calculated from iodometric back titration = 0.22695g

Percentage of pure caffeine

= (0.22695÷0.347) × 100 = 65.40%

Table 2: Iodometric back titration for caffeine extracted from the tea leaves *Nalari Gold*

(Amount extracted from 10 grams of NLR is 0.224g)

Sl no.	Sample Nalari Gold (mL) (0.02307 mol)	Volume of H_2SO_4 (mL) (0.05 mol)	Volume of I_2 (mL) (0.05 mol)	Volume of $Na_2S_2O_3$ (mL) (0.005 mol)
1	10	10	10	7.6
2	10	10	10	7.6
3	10	10	10	7.6
4	10	10	10	7.7

Calculations:

Amount of crude caffeine extracted (NLR) and taken for estimation = 0.224g

Concentration of caffeine = 0.02307 mol (0.224g in 50 mL)

Volume of caffeine taken for titration = 10 mL

Volume of I_2 added = 10 mL

No. of moles of I_2 added = (10 ÷ 1000) × 0.05 mol = 5×10^{-4} mol

No. of moles of $Na_2S_2O_3$ = (7.6 ÷ 1000) × 0.005 mol = 3.8×10^{-5} mol

From the equation:

$$I_2 + 2Na_2S_2O_3 \longrightarrow 2NaI + Na_2S_4O_6$$

No. of moles of I_2 reacted with $Na_2S_2O_3$ (excess I_2) = 3.85×10^{-5} mol /2 = 1.9×10^{-5} mol

Therefore, number of moles of I_2 reacted with caffeine = (total iodine added – excess iodine)

= 5×10^{-4} mol - 1.9×10^{-5} mol = 3.1×10^{-4} mol

From the equation:

$$C_8H_{10}N_4O_2 + 2I_2 + KI + H_2SO_4 \longrightarrow C_8H_{10}N_4O_2{\cdot}HI{\cdot}I_4 + KHSO_4$$

Number of moles of caffeine reacted with iodine = 3.1×10^{-4} mol/2 = 1.55×10^{-4} mol. Therefore, amount of caffeine in 10 ml = 1.55×10^{-4} mol ×194.19 g/mol = 0.03009945 g

Thus, amount of caffeine in 50 ml = 0.03009945×5 = 0.150497g

Amount of crude caffeine taken (*Nalari Gold*) = 0.224 g

Amount of caffeine calculated from iodometric back titration = 0.150497g

Percentage of pure caffeine = (0.150497g ÷ 0.224) ×100 = 67.39%

4. CONCLUSION

Caffeine has been extracted successfully from the two local tea brands *Namar Jongphi* and *Nalari Gold* Tea leaves following the liquid-liquid extraction method. The quantitative analysis of the extracted caffeine was successfully carried out using the iodometric back titration. The amount of crude caffeine extracted from 10 grams of *Namar Jongphi* and *Nalari Gold* tea leaves was 0.347g and 0.224g, respectively. Following the stoichiometric calculations for the determination of caffeine by iodometric method, the amount of pure caffeine present in *Namar Jongphi* tea leaves was 0.22695g with the percentage of crude over pure caffeine calculated to be 65.40%. The amount of caffeine estimated from the

Nalari Gold tea leaves calculated was 0.150497g with percentage of recovery 67.39%.

ACKNOWLEDGEMENT

We express our gratitude to the Department of Chemistry, NEHU for the IR analysis and we are indebted to the Head of the Department of Chemistry for her constant support and encouragement. We would also like to thank the Head of the Department of Zoology, for granting us the permission to use instruments like centrifuge, etc.

REFERENCES

[1] Rodak, K., Kokot, I., & Kratz, E. M. (2021). Caffeine as a factor influencing the functioning of the human body-friend or foe? *Nutrients*, *13* (3008), 1-29.

[2] Mahoney, C. R., Giles, G. E., Marriott, B. P., Judelson, D. A., Glickman, E. L., Geiselman, P. J., & Lieberman, H. R. (2019). Intake of caffeine from all sources and reasons for use by college students. *Clin. Nutr*, *38,* 668–675.

[3] Heckman, M. A., Weil, J., & De Mejia, E. G. (2010). Caffeine (1, 3, 7-trimethylxanthine) in Foods: A comprehensive review on consumption, functionality, safety, and regulatory matters. *J. Food Sci*, *75*, 77–87.

[4] Kolahdouzan, M., & Hamadeh, M. J. (2017). The neuroprotective effects of caffeine in neurodegenerative diseases. *CNS Neurosci. Ther*, *23*, 272–290.

[5] Pohanka, M., & Dobes, P. (2013). Caffeine inhibits acetylcholinesterase, but not butyrylcholinesterase. *Int. J. Mol. Sci*, *14,* 9873–9882.

[6] Onami, T., & Kanazawa, H. (1996). A simple method for isolation of caffeine from black tea leaves: Use of a dichloromethane-alkaline water mixture as an extractant. *J. Chem. Educ*, *76(6)*, 556.

[7] Madureira, A. M., Vieira Abel, J. S. C., & Ferreira, M-J. U. (2017). Caffeine extraction from tea and coffee. *In* "comprehensive organic chemistry experiments for the laboratory classroom, *Royal Society of Chemistry."*

[8] Rebecca, L. J., Seshiah, C., & Tissopi, T. (2014). Extraction of caffeine from used tea leaves. *The Annals of "Valahia" University of Targoviste.*

[9] Chaugule, A., Patil, H., Pagariya, S., & Ingle, P. (2019). Extraction of caffeine. *Int. j. adv. res. chem. sci, 6(9)*, 11-19.

[10] Shinde, R. R., & Shinde, S. H. (2017). Extraction of caffeine from coffee and preparation of anacin drug. *Int. J. Eng. Res. Technol*, *10(1),* 236-239.

[11] Bhailume, M. V., & Shinde, S. (2020). Quantitative analysis of caffeine by percent degradation assay and iodometric titration. *Int. J. Sci. Res*, *9(12),* 288-290.

[12] Kalsi, P. S. (2002). Spectroscopy of Organic Compounds. New Age International Publishers, New Delhi.

Research article:

DFT study of VO_2 and Ag-VO_2: Band structure and Density of state

Pushpendra Singh Shekhawat, Umesh K. Dwivedi and Sandip Paul Choudhury*

Amity School of Applied Science, Amity University, Rajasthan, India

Article Info:
https://doi.org/10.54290/spect/2022.9.1.0005

Received: November 18th, 2022
Revised: November 21st, 2022
Accepted: November 24th, 2022

****Corresponding author:***
sandip.pchoudhury@gmail.com

Abstract: In this work we have studied the electronic properties of VO_2 by employing the density functional theory (DFT). The CASTEP module was used for the simulation. 2x2x1 lattice of VO_2 was used for study of the band structure and density of state. The electronic properties change significantly on doping the sample with Ag. Also, when Ag is doped in different quantities in VO_2, the bad gap is not the same as that of pure VO_2 and the conductivity and dielectric constant also changes.

Keywords: DFT, Ag-VO_2, VO_2, Electronic properties, Band Structure, Density of State

1. INTRODUCTION

In the past years the study of vanadium oxide (VO_2) has attracted a lot of attention due to its strong relativity to electronic materials, when the phase transition temperature (T_c) is more than 68°C, it shows a metal-semiconductor transition to rutile phase from monoclinic phase [1]. VO_2 has a potential as smart window coatings, optical switches and gas sensors devices due to a reversible change in electronic and optical properties by phase transition [2-7]. However, the phase transition temperature of 68°c limits the practical application of VO_2 and to overcome this limitation, elemental doping is introduced and found to be the most effective way to lower phase transition temperature. Basically, the V-V bonding range in VO_2, which is essential for the phase transition, may be changed by the elemental doping, and this would affect phase transition temperature [8]. Numerous studies with elementally doped VO_2 are carried out successfully. For instance, it is simple to lower the phase transition temperature of W-doped VO_2 to ambient temperature

How to Cite:
Shekhawat et al.(2022). DFT study of VO2 and Ag-VO2: Band structure and Density of state. *Spectrum: Science and Technology, v9 (1), 43-49.* https://doi.org/10.54290/spect/2022.v9.1.0005

[9]. The Fermi level may shift toward the conduction band in the presence of Mo donors, which would cause the activation energy Ea and then phase transition temperature to fall [10]. Mg-doped VO_2 can lower Tc and increase visual transmittance [11]. VO_2 can also be doped with lanthanides, such as La and Tb, to lower the Tc because of their abundant valence electrons and large ionic radii [12]. Y-R Jo et al. [13] worked on electron-doped VO_2 and reported that the creation of a transmission electron microscopy (TEM) grid with the ideal configuration of Si_3N_4 windows that may safely be used for photolithography of individual electron-doped VO_2 nanowire devices, enabling a comparison of their structural and electrical characteristics. Quantitative analysis of the rutile and M1 phase fractions was done using TEM dark-field imaging, and their lattice alignments were seen using high-resolution TEM (HRTEM) with small area diffraction. Elkady et al. [14] Synthesized nano $VO_2 \cdot 0.5\ H_2O/ZrV_2O_7$ and doped with Cs, Cr and Ga using combined precipitation-hydrothermal that followed by gentle heating at low temperature and described and examined the growth mechanism of doping using XRD, SEM, TEM, Raman, TGA, DSC, and UV-vis spectroscopy. And resulted that all composites have a negative thermal coefficient between 25 and 100 and a positive thermal coefficient between 100 and 300 . Zhao et al. [15] reported that the Vanadium dioxide's metal-insulator transition (MIT) and physical characteristics may be tuned effectively by ion doping (VO_2). With various W concentrations and applied voltages, the fluctuation of electrical conductivity of W-doped VO_2 was studied. The conductivity of W-doped VO_2(R) is poorer without an external electric field than that of undoped VO_2(R), and it gets worse as the W concentration rises. Wang et al. [16] investigated that possibility to create single crystalline W-doped VO_2 nanobeams for use in electrical and optical systems. And resulted that Dual surface plasmon resonance peaks at 1344 and 619 nm are produced as a result of variations in the polarisation of the beams along their transverse and longitudinal axes, which increases the VO_2 nanobeams' capacity to modulate solar radiation. One of the finest noble metals for thermal and electrical conductivity is silver. Zhou et al. [17] included Ag particles periodic arrays into VO_2(M) films by using self-assembling polystyrene (PS) templates with a hexagonal-close-packed monolayer as the mask. Ag particles periodic arrays (PPAs) with various specific areas were produced in the VO_2(M) films by adjusting the size of PS nanospheres. As a result, it was discovered that the Tc was lowered from 68 to 57.5 C and that the carrier density had increased due to the larger specific area. More free electrons injected into VO_2(M) films resulted in a bigger absorption energy at the internal junction, according to a detailed mechanism of Tc reduction that combined with the analysis of the energy band of Ag/VO_2(M). The significantly improved Ag PPAs/VO_2(M) films satisfy the requirements of a lowered T_c and diluted colour simultaneously, making them appropriate for commercial usage in energy-efficient glass.

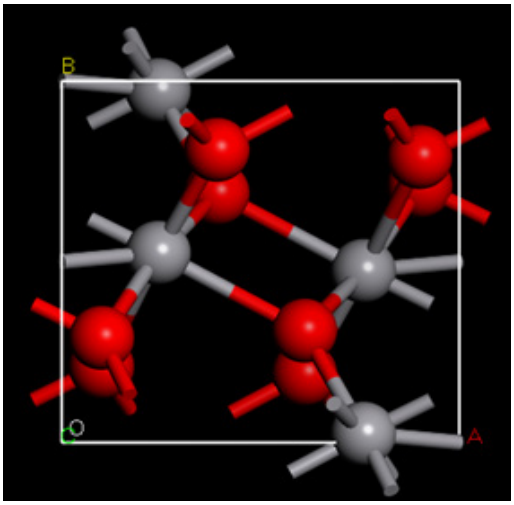

Figure 1. Crystal structure of VO_2

This study used the DFT approach to examine the electrical structures of pure VO_2 as well as Ag-doped VO_2 at different concentrations of Ag, including the energy gap and density of states. This research can shed crucial light on the process by which doping techniques can alter the structure of VO_2.

2. COMPUTATIONAL DETAILS

This computation was performed using the CASTEP software (Cambridge sequential total energy package). The crystal structure optimised by the molecular dynamics module serves as the foundation for DFT calculations. The exchange-correlation functional of the Perdew-Wang 91 (PW91) generalized-gradient-approximations (GGA) was employed. Ultrasoft pseudopotentials served as a representation for the interactions between the ionic core and the valence electrons. On the basis of the previous findings [18], a uniform Monkhorst-Packard k grid with a 1 x 1 x 1 spacing was chosen for the M1 phase. The adopted values of U were set at 2.5 eV for the vanadium d electrons in our simplified application of the rotationally invariant LDA+U technique. The atomic energy convergence criteria for the BFGS method is 1-10 eV/atom, the atomic force convergence criteria is 0.05 eV/nm, the crystals stress convergence threshold is 0.05 GPa, and the atomic maximum displacement convergence criteria is 0.001. The space group of the M1 phase VO_2 is P21/c.

The relative lattice constants are 5.734, 4.517, and 5.375. Each oxygen atom coordinates with an adjacent three vanadium atoms, while each vanadium atom coordinates with an adjacent six oxygen atoms and one vanadium atom (Fig. 1). The supercell method (2 x 2 x 2) was used to model the Ag/VO_2 model, which was produced from the optimal unit cell and is depicted in Fig. 2. Supercell VO_2 was calculated to determine the electrical structure and optical characteristics of undoped VO_2 for comparison.

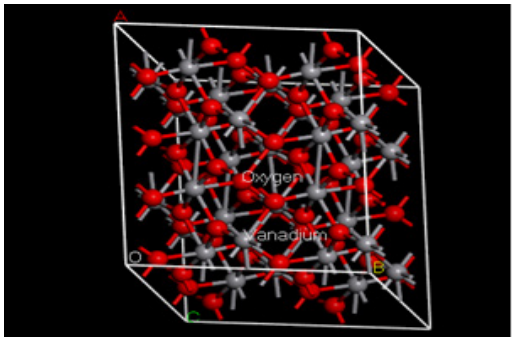

Figure 2. Supercell of VO_2

3. RESULTS AND DISCUSSION

3.1 Band structure

The band structures of VO_2 and Ag/VO_2 and Ag_2/VO_2 are depicted in Figures 3(a), 3(b) and 3(c) respectively. The band gaps of VO_2 and Ag/VO_2 are, respectively, 0.115 eV, 0.024 eV and the

band gap for the higher concentration doping was not given by the calculations as the conduction band and valance band overlaps, which are low compared to the theoretical value (0.7 eV). DFT in GGA functional, which is inadequate to process inter-electron exchange interactions and has no impact on the analysis of energy gap data, resulting in smaller band gap values. In other words, the Ag doped VO_2 band gap is significantly narrower than the band gap of pure VO_2, indicating that the doped VO_2 has a higher metallicity.

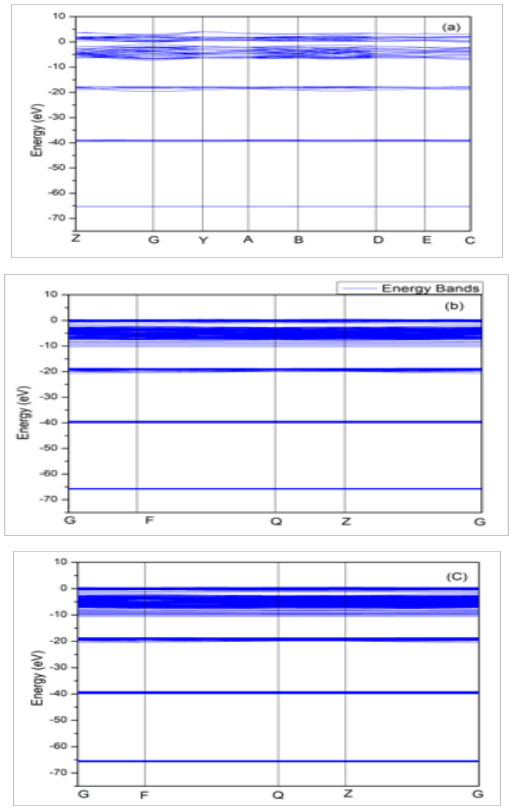

Figure 3. Energy band structure of VO_2, Ag/VO_2 and Ag_2/VO_2

3.2 Density of states

The total densities of the VO_2 and Ag doped VO_2 states are displayed in Fig. 4. The total density of states curves for VO_2 and Ag doped VO_2 are quite similar, as seen in Fig. 4. The partial densities of the states of the V atom for VO_2 (a) and the Ag atom for Ag doped VO_2 are shown in Fig. 5. (b) and 5. (c). The vanadium atom's density of states is mostly composed of four groups. The first group comes from the V 4s orbital and is between -67 and -65 eV. The second group, from the V 4p orbital, lies between -40 and -37 eV. In the third group, which spans the energy range of -7 to 0 eV, V 3d orbitals predominate. V 3d orbitals make up the conduction band.

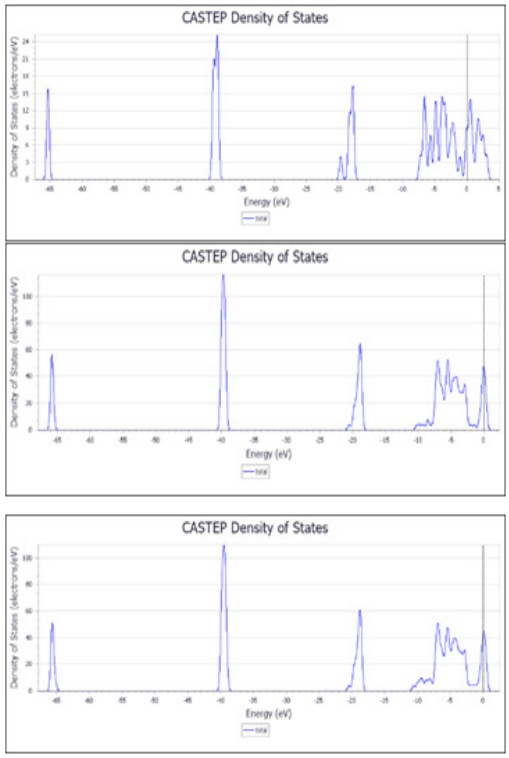

Figure 4. Total density of states for VO_2, Ag/VO_2 and Ag_2/VO_2

Figure 5 also depicts the results of

the DOS for interactions between vanadium and oxygen for VO_2, and silver and oxygen for Ag/VO_2. Near the Fermi level, O 2p interacts with V 3d mostly for VO_2, whereas O 2p interacts with Ag 4d primarily for Ag/VO_2. Near the Fermi level, O 2p interacts with V 3d mostly for VO_2, whereas O 2p interacts with Ag 4d primarily for Ag/VO_2.

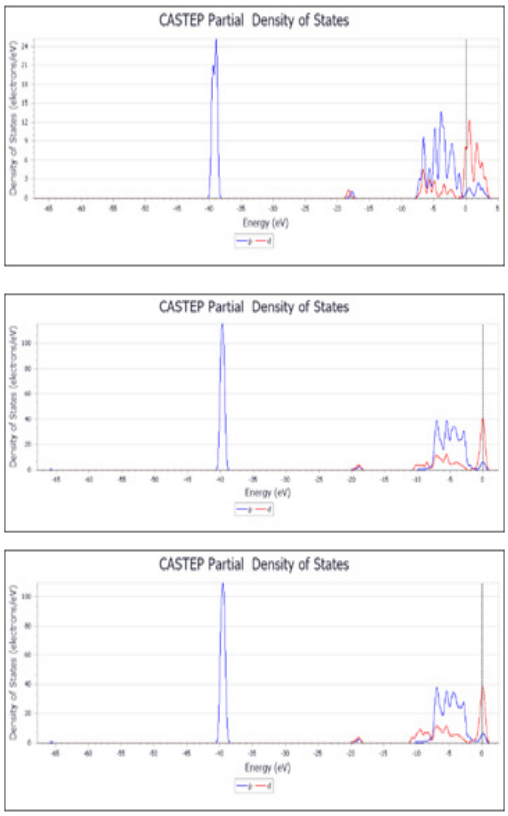

Figure 5. Partial density of states for VO_2, Ag/VO_2 and Ag_2/VO_2

Silver is more active than vanadium, as evidenced by the fact that the DOS of Ag 4d for Ag-O is greater than that of V 3d for V-O bond. Additionally, compared to O 2p and V 3d orbitals, Ag4d and O 2p orbitals overlap more widely. These findings demonstrate that oxygen interacts with silver more strongly than it interacts with vanadium.

4. CONCLUSION

By using the DFT approach, the electrical structure, and optical characteristics of VO_2, Ag/VO_2 and Ag_2/VO_2 were investigated. In comparison to V and O, Ag and O interact more strongly. In the Ag–O connection, there is both ionic and covalent bonding. Ag/VO_2 and VO_2 have respective band gaps of 0.115 eV and 0.024 eV. In other words, when Ag is doped in VO_2, the band gap shrinks while the conductivity increase.

REFERENCES

[1] Morin, F. J. (1959). Oxides which show a metal-to-insulator transition at the Neel temperature. *Physical review letters*, *3*(1), 34.

[2] Wang, S., Liu, M., Kong, L., Long, Y., Jiang, X., & Yu, A. (2016). Recent progress in VO2 smart coatings: Strategies to improve the thermochromic properties. *Progress in Materials Science*, *81*, 1-54.

[3] Fu, H., Xie, H., Yang, X., An, X., Jiang, X., & Yu, A. (2015). Hydrothermal synthesis of silver vanadium oxide (Ag0. 35V2O5) nanobelts for sensing amines. *Nanoscale research letters*, *10*(1), 1-12.

[4] Yang, X. H., Fu, H. T., An, X. Z., Jiang, X. C., & Yu, A. B. (2016). Synthesis of V 2 O 5@ TiO 2 core–shell hybrid composites for sunlight degradation of methylene blue. *RSC advances*, *6*(41), 34103-34109.

[5] Liu, M., Su, B., Kaneti, Y. V., Chen, Z., Tang, Y., Yuan, Y., ... & Yu, A. (2017). Dual-phase transformation: Spontaneous self-template surface-patterning strategy for ultra-transparent VO2 solar modulating coatings. *Acs Nano*, *11*(1), 407-415.

[6] Ke, Y., Zhou, C., Zhou, Y., Wang, S., Chan, S. H., & Long, Y. (2018). Emerging thermal-responsive materials and integrated techniques targeting the energy-efficient smart window application. *Advanced functional materials*, *28*(22), 1800113.

[7] Ke, Y., Wen, X., Zhao, D., Che, R., Xiong, Q., & Long, Y. (2017). Controllable fabrication of two-dimensional patterned VO2 nanoparticle, nanodome, and nanonet arrays with tunable temperature-dependent localized surface plasmon resonance. *ACS nano*, *11*(7), 7542-7551.

[8] Goodenough, J. B. (1971). The two components of the crystallographic transition in VO2. *Journal of Solid State Chemistry*, *3*(4), 490-500.

[9] Chen, R., Miao, L., Liu, C., Zhou, J., Cheng, H., Asaka, T., ... & Tanemura, S. (2015). Shape-controlled synthesis and influence of W doping and oxygen nonstoichiometry on the phase transition of VO2. *Scientific reports*, *5*(1), 1-12.

[10] Mai, L. Q., Hu, B., Hu, T., Chen, W., & Gu, E. D. (2006). Electrical property of Mo-doped VO2 nanowire array film by melting– quenching sol–gel method. *The Journal of Physical Chemistry B*, *110*(39), 19083-19086.

[11] Hu, S., Li, S. Y., Ahuja, R., Granqvist, C. G., Hermansson, K., Niklasson, G. A., & Scheicher, R. H. (2012). Optical properties of Mg-doped VO2: Absorption measurements and hybrid functional calculations. *Applied Physics Letters*, *101*(20), 201902.;

[12] Wang, N., Shun, N. T. C., Duchamp, M., Dunin-Borkowski, R. E., Li, Z., & Long, Y. (2016). Effect of lanthanum doping on modulating the thermochromic properties of VO 2 thin films. *RSC advances*, *6*(54), 48455-48461.

[13] Jo, Y. R., Kim, M. W., & Kim, B. J. (2016). Direct correlation of structural and electrical properties of electron-doped individual VO2 nanowires on devised TEM grids. *Nanotechnology*, *27*(43), 435704.

[14] Elkady, M., Hamad, H., & El Essawy, N. (2019). Modification of optical and electrical properties of nanocrystalline VO2· 0.5 H2O/ZrV2O7: influence of Cs, Cr and Ga doping. *Journal of Materials Research and Technology*, *8*(1), 1212-1223.

[15] Zhao, Z., Li, J., Ling, C., Zhao, X., Zhao, Y., & Jin, H. (2021). Electric field driven abnormal increase in conductivity of tungsten-doped VO2 nanofilms. *Thin Solid Films*, *725*, 138643.

[16] Wang, N., Duchamp, M., Xue, C., Dunin-Borkowski, R. E., Liu, G., & Long, Y. (2016). Single-crystalline W-doped VO2 nanobeams with highly reversible electrical and plasmonic responses near room temperature. *Advanced materials interfaces*, *3*(15), 1600164.

[17] Zhou, Z., Li, J., Xiong, Z., Cao, L., Fu, Y., & Gao, Z. (2020). Reducing transition temperature and diluting brown-yellow color of VO2 films via

embedding Ag particles periodic arrays. Solar Energy Materials and Solar Cells, *206*, 110303.

[18] Zhang, X. R., Wang, W., Zhao, Y., Hu, X., Reinhardt, K., Knize, R. J., & Lu, Y. (2012). Temperature-agile and structure-tunable optical properties of VO2/Ag thin films. *Applied Physics A*, *109*(4), 845-849.

[19] Joushaghani, A., Jeong, J., Paradis, S., Alain, D., Stewart Aitchison, J., & Poon, J. K. (2014). Voltage-controlled switching and thermal effects in VO2 nano-gap junctions. *Applied Physics Letters*, *104*(22), 221904.

Research article:

Study on Soil nutrients of some selected areas of Khasi and Jaintia Hills of Meghalaya with reference to Scientific Fish farming

Rupak Nath and Wanshaphrang Tiewsoh

Department of Fishery Science, St Anthony's College, Shillong, India

Article Info:
https://doi.org/10.54290/spect/2022.v9.1.0006

Received: November 1st, 2022
Revised: November 15th, 2022
Accepted: November 20th, 2022

Corresponding author:
nathrupak10@gmail.com

Abstract: Good quality soil is very important for better productivity in the fish farm. Some areas of Khasi and Jaintia Hills District were selected to collect soil sample and analysed to check suitability for fish farming. The soil analysis of the selected areas reveals that soils are highly acidic in nature and deficient in available nitrogen and phosphorus. Proper treatment with lime, nitrogen and phosphorus based fertilizers are required to enhance the productivity of fish farm. Soil texture of the study areas was found sandy loam to clay loam which indicates suitability of the areas for construction of fish farm.

Keywords: *Khasi hills, soil nutrients, lime, phosphorus, nitrogen, fish farming*

1. INTRODUCTION

The state Meghalaya lies 20^0 1/ N - 20^0 5/ N latitude and 85^0 49/ E - 92^0 52/ E longitude, occupies 22,428 sq.km, which is 9.3% of the total geographical area of the North East Region of India. The state is physiographically divisible into Eastern Meghalaya (Jaintia Hills), Central Meghalaya (Khasi Hills) and Western Meghalaya (Garo Hills) [1]. The total geographical area of Khasi Hills is 1044764 ha which includes five districts namely East Khasi Hills, West Khasi Hills, South West Khasi Hills, Eastern West Khasi Hills and Ri-Bhoi district. Altitude of Khasi Hills varies from 150m msl to 1960m msl Khasi Hills is cooler than Garo Hills where maximum temperature goes up to 25^0C as compared to 35^0C in Garo Hills during summer season [1, 5].

The quality of soil is important in fish farms, due to its influence on productivity and the quality of the overlying water, but also because of

How to Cite:
Nath R and Tiewsoh W (2022). Study on Soil nutrients of some selected areas of Khasi Hills with reference to Scientific Fish farming. *Spectrum: Science and Technology, v9 (1), 51-56.* https://doi.org/10.54290/spect/2022.v9.1.0006

its suitability for dike construction. Sandy clay to clay loam soils are considered suitable for pond construction. Because of their cohesive properties, the fine-textured soils (clay, silty clay, clay loam, silty clayloam and sandy clay) are more suitable for pond construction for fish farms [11]. Soil plays an important role in determining the fertility of fish ponds. Primary nutrients, mainly nitrogen (N), Phosphorus (P) and Potassium (K) are playing vital roles in pond productivity [10, 8]. Soil with clay content less than 18 % (sandy/Silty) in soil can be used for fish culture with treatment but too sandy and silty soil are totally unfit for excavation of pond due prevailing excessive seepage problem.

The soils of upper reaches of Shillong plateau are red loam. The soils are uniformly deficient in available phosphorus which in due to acidic reaction. The soils vary from sandy loam to clay loam and acidic in reaction with high aluminium and iron content. Majority of the acid soils in Meghalaya have pH 4.7 – 5.4 (1). Nath, 2010 [9] stated that development of package of practices for composite and integrated fish farming is utmost important for the development of aquaculture in Meghalaya.

2. MATERIALS AND METHODS

Soil sampling was carried out by adopting methodology given by M.R. Carter and E.G. Gregorich and Jackson,1973 [7, 12], Canadian Society of Soil Science. Soil samples were collected from sample depth 0 to 30 cm. All samples from one sub section are combined and a composite sample was made. Selection and collection soil sample was done by the Benchmark Sampling. In this design a single representative site (benchmark) was selected for each field or subsection of a field. 6 samples were randomly taken from within the benchmark and then composited for laboratory analysis. Composite sampling was prepared and analysed in the ICAR- Research complex for NEH Region, Umiam, Meghalaya. To assess productivity of the study areas with reference to nutrient values in soil sample like OC%, available nitrogen and available phosphorus, a comparison were made with soil productivity reference given by the CIFRI,1985 [3]

3. RESULTS AND DISCUSSION

Soil texture of Khasi and Jaintia hills were found to be sandy loamy at Pynursla to Clay loamy at Pynthurba (Table1).

Table1: Soil texture in the study area

Sources of the samples		Texture
East Khasi Hills	Mawli	Silt loam
	Pynursla	Sandy loam
	Pymthurba	Clay loam
	Smit 1	Silt loam
	Smit 2	Clay loam
	Sohra	Sandy loam
Jaintia Hills	Dawki	Sandy loam
	TLUH Village	Silty clay loam
Ribhoi	Raithong	Silt loam
	Umsohliet	Loam

Soil pH of the study area were shown acidic in nature which varies

from 3.83 (Mawli and Umsohliet) to 5.38 (Sohra) (Table 2).

Table 2: Productivity of soil with reference to pH

Sl No.	Sources of the samples	pH (1:2.5)		
1.	East Khasi Hills (Mawli)	3.83	Highly acidic	Low productive
2.	East Khasi Hills, Pynursla	4.00	Highly acidic	
3.	East Khasi Hills, Pynthurba	5.33	Moderately acidic	
4.	East Khasi (SMIT) Hills	4.54	Highly acidic	
5.	East Khasi Hills, SMIT	5.00	Moderately acidic	
6.	East Khasi Hills, Sohra	5.38	Moderately acidic	
7.	Jaintia Hills (Dawki)	4.27	Highly acidic	
8.	Jaintia Hills, TLUH Village	4.11	Highly acidic	
9.	Ribhoi Raithong	3.91	Highly acidic	
10.	Ribhoi, Umsohliet	3.83	Highly acidic	

In case of Organic Carbon (OC %) maximum areas under study was found high to moderate content of organic carbon indicates good productivity (Table 3).

Table 3: Productivity of soil with reference to Organic carbon

Sl No.	Sources of the samples	OC (%)	
1.	East Khasi Hills (Mawli)	2.54	Highly productive
2.	East Khasi Hills, Pynursla	0.23	Low productive
3.	East Khasi Hills, Pymthurba	0.94	Low productive
4.	East Khasi Hills (Smit)	2.15	Highly productive
5.	East Khasi Hills, (Smit)	2.26	Highly productive
6.	East Khasi Hills, Sohra	0.90	Low productive
7.	Jaintia Hills (Dawki)	0.16	Low productive
8.	Jaintia Hills, Tluh Village	1.37	Medium productive
9.	Ribhoi Raithong	1.17	Medium productive
10.	Ribhoi, Umsohliet	2.65	Highly productive

Important nutrients which determine productivity of soil namely available nitrogen and phosphorus was found deficient in the study areas which indicates low productivity (Table 4 & Table 5).

Table 4: Productivity of soil with reference to nitrogen

Sl No.	Sources of the samples	Av. N mg/100g	
1.	East Khasi Hills (Mawli)	24.285	Low productive

2.	East Khasi Hills, Py-nursla	16.000	Low productive
3.	East Kha-si Hills, Pymthurba	12.054	Low productive
4.	East Khasi (SMIT) Hills	19.642	Low productive
5.	East Khasi Hills, SMIT	20.982	Low productive
6.	East Khasi Hills Sohra	13.169	Low productive
7.	Jaintia Hills (Dawki)	10.714	Low productive
8.	Jaintia Hills, TLUH Vil-lage	15.178	Low productive
9.	Ribhoi Rai-thong	11.161	Low productive
10.	Ribhoi, Um-sohliet	25.000	Low productive

Table:5 Productivity of soil with reference to Phosphorus

Sl No.	Sources of the samples	Av. P mg/100g	
1.	East Khasi Hills(Mawli)	0.97	Low productive
2.	East Khasi Hills, Pynursla	0.62	Low productive
3.	East Kha-si Hills, Pymthurba	0.68	Low productive
4.	East Khasi Hills Smit	0.88	Low productive
5.	East Khasi Hills, SMIT	0.81	Low productive
6.	East Khasi Hills Sohra	0.47	Low productive
7.	Jaintia Hills (Dawki)	0.45	Low productive
8.	Jaintia Hills, TLUH Village	0.72	Low productive
9.	Ribhoi Raithong	0.58	Low productive
10.	Ribhoi, Umsohliet	0.81	Low productive

Fig 1: Chemical properties of Soil of Khasi and Jaintia Hills

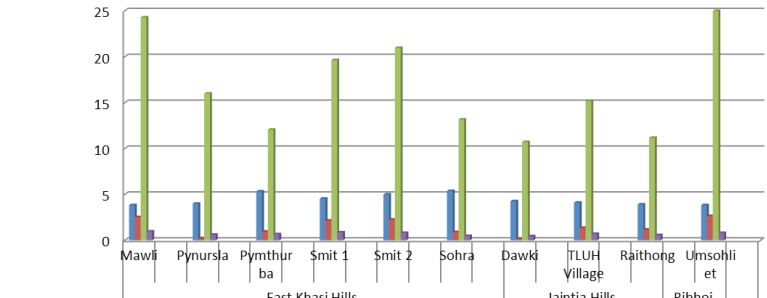

Available nitrogen and phosphorus was ranging from 10.714 mg/100 g to 24.285 mg/100g soil and 0.45 mg/100 g to 0.97 mg/100 g soil respectively (Fig 1).

Soil textures of the study area are falls under the range of sandy loam (15% clay) to clay loam (35% clay) which indicates suitability for fish cultivation. Pillay *et al*, 2005 [10], stated that the fine- textured soils like clay, silty clay, clay loam, silty clay loam and sandy clay) are more suitable for pond farms. Soil sample analysed from the different locations of the study areas reveals that soils are moderate to highly acidic in nature and falls under the low productive category. Low soil pH may be due high rainfall in the study areas which is responsible of leaching out basic cations and leave behind acids (Al and H) [8]. Soils under study area were found low productive with regards to available nitrogen and phosphorus which is confirmation of study CIFRI, 1985. Organic carbon was recorded in wide ranges in the study areas i.e low, medium to high level (Table 3). As per recommendation of package of Practices on carp culture by CIFRI the suggested lime dose (Agricultural lime stone $CaCo_3$) to neutralize acidity would be 2000 kg/ha/year. Deficiency of nitrogen and phosphorus in fish farm can be overcome by applying Urea @ 225-290 kg/ha/year and Single Super Phosphate (SSP) @ 315-405 kg/ha/year respectively [3].

4. CONCLUSION

Location specific aquaculture is more appropriate than the conventional aquaculture to achieve sustainable development in aquaculture sector. Development of appropriate location specific aquaculture technology and packages of practices on scientific fish farming is the need of the hour to accelerate fish production in Meghalaya. It is advisable that before starting fish culture, the soil should be tested and treatment should be given accordingly to enhance fish production.

REFERENCES

[1] Das A, Ghosh P.K, Choudhury B.U, Patel D. P, Munda G. C, Ngachan S. V and Chowdhury P (2009). Climate change in northeast India: recent facts and events – worry for agricultural management: *ISPRS Archives XXXVIII-8/W3 Workshop Proceedings.*

[2] Das P and Sinha M (1985). Carp seed Raising package of practices for increasing carp seed production, *Aquaculture extension manual, series 1, CIFRI, Barrackpore.*

[3] Sinha, V. R. P Chakraborty, R. D, Tripathi, S. D, Das, P & Sinha, M (1985). Carp Culture package of practices for increasing carp *production, Aquaculture extension manual, series 1, CIFRI, Barrackpore.*

[4] Gupta, A.D and Kapoor, A.N., (1999). Principle of physical Geography: *A Text Book of Physiography.* S. Chand and Company Ltd. NewDelhi-110055.

[5] Khan. A. R and Alfred. J. R. B., (1995). Ecology and General Faunal Resources of some Wetlands in Garo hills. In: *Fauna of Meghalaya, Part1, Vertebrates, State Fauna Series 4, Zoological Survey of India.*

[6] M. R. Carter and E. G. Gregorich (2006) Soil Sampling and Methods of Analysis.

Canadian Society of Soil Science. Taylor & Francis Group, LLC

[7] Mookerjee, H. Ganguly. D. N and Sen Gupta. S. N (1946) The optimum range of temperature of water for the fingerlings of major carps of India. *Sci Cult. -11*

[8] Miller, J, O (2016). Soil pH Affects Nutrient Availability, university of Maryland extension.

[9] Nath. R (2010) Current status and strategies for sustainable development of fisheries sector in Meghalaya. In *Mahanta et al., eds.* ICAR-DCFR Publications, Bhimtal.

[10] Pillay. T. V. R and Kutty. M. N (2005). Aquaculture - Principle and Practices, *Blackwell Publishing Ltd, 9600 Garsington Road, Oxford OX4 2DQ, UK*

[11] Sinha VRP and Ramachandran. V (1985). *Fresh water Aquaculture,* ICAR, New Delhi.

[12] Jackson, M.L. (1973). *Soil Chemical Analysis*. Prentice Hall of India Pvt Ltd., New Delhi.

Short Communication:

A study of the ITK used in fisheries and Bioresources of Lai Lyngdoh area, West Khasi Hills, Meghalaya

Jylliewkupar Kharbani[1] and Jasmine T. Sawian[1]*

[1]Department of Environmental Science,
St. Edmund's College, Shillong 793003, Meghalaya, India

Article Info:
https://doi.org/10.54290/spect/2022.v9.1.0007

Received: July 10th, 2022
Revised: October 10th, 2022
Accepted: October 20th, 2022

Corresponding author:
jsawian@gmail.com

Abstract: Indigenous traditional knowledge (ITK) has been in use different districts of Meghalaya and it is of different types. In West Khasi hills of district few important ITK is used especially in connection with fish. Besides ITK, bioresources are seen to play an important role in the lives of indigenous communities in Lai Lyngdoh area. The Lai Lyngdoh area in Nongstoin is a group of 34 villages that falls under the jurisdiction of the three Lyngdoh i.e. Marskuin, Nonglwai and Nongkhlaw located in West Khasi Hills District, Meghalaya. The locals in the area mostly depend on the surrounding environment for their livelihood. From the surrounding forests and forest streams, a variety of minor products are harvested and a number of edibles which include wild fruits, leafy green, wild vegetables, mushroom, fish, frog, crustaceans, tubers and medicinal plants are also gathered. Indigenous traditional knowledge (ITK) in the use of bio-resources is still preserved and practised in the indigenous communities and the documentation of local culture and knowledge will play an important role in conservation process. These resources, however, need to be valued and used sustainably so that they can continue to support the community.

Keywords: *Indigenous traditional knowledge (ITK), Bio-resources, Lai Lyngdoh, indigenous knowledge, sustainable use.*

1. INTRODUCTION

Biological resources include all products and services emanating from natural environment that satisfies the needs and wants of human. The purpose of bio-resources is to provide a sustainable response to the need of food

How to Cite:
Kharbani and Sawian (2022). A study of the ITK used in fisheries and Bioresources of Lai Lyngdoh area, West Khasi Hills, Meghalaya. *Spectrum: Science and Technology, v9 (1), 57-68.* https://doi.org/10.54290/spect/2022.v9.1.0007

and to part of society's requirements for materials and energy, as well as providing society with ecosystem services [2]. The basic component of any country knowledge system is its indigenous knowledge. It encompasses the skill, experience and insights of people and is applied to sustain, improve their livelihood [6]. Communities in developing countries greatly rely on indigenous natural resources or bio-resources, which play an important role in income generation. Ethnic group across the global possess tremendous amount of traditional knowledge, most of which are poorly documented and hence are largely unknown [4]. Recording such knowledge is pivotal before they get lost forever in the fast push for modernization and globalization.

Fishers of India have a rich legacy of indigenous knowledge, traditional practices and customary rules and regulations. It is widely acknowledged that traditional knowledge of fishers and their community-based management systems hold immense value for sustainable fisheries management. Over thousands of years, traditional fishing communities in many parts of the world have evolved numerous social systems often unwritten to regulate their fisheries and maintain biological diversity. There is a need to understand, respect and tap these social resources for better governance of fisheries. Careful documentation of this knowledge will provide essential elements to formulate management plans towards ecologically sustainable development. In the recent times, there is a growing interest in the role that ITK systems play in development. Research is generating data showing the relevance of IK as a resource that provides a basis for sustainable and environmentally sound approaches to fisheries and natural resource management. It is widely acknowledged that traditional knowledge of fishers and their community-based management systems hold immense value for sustainable fisheries management

The role of indigenous traditional knowledge in fulfilling the objectives of biodiversity conservation; and to recognize the consequences of climate change at small scales is gaining importance in the current mainstream conservation models. Traditional resource management systems are considered to be unbiased system and often ensure equitable sharing of benefits forest and other natural resources [1, 3]. However, over exploitation of biological resources along with excessive habit change constitutes one of the major worldwide threats to wildlife. In the tropic, this problem acquires greater significance with high human population and the greater dependence of human bio-resources for subsistence and profiteering [5].

Like many indigenous communities, the villages in Nongstoin, West Khasi Hills, has a long tradition of natural resources conservation based on custom and religious belief that has been passed on from generation to another. However, very less attempts have been made so far to document these natural resources. Very little data is available on the types of resources and services the areas have to offer; and many a times; they are either overexploited or not put to use at all, with evidence of lack of proper management. The present study, therefore, aim to

document the diversity of bio-resources in the area and the indigenous traditional knowledge practised in the use and conservation of the biological resources which may play an important role in the conservation and management forest and land resources of the areas.

2. MATERIALS AND METHODS

The study is conducted in Lai Lyngdoh area in Nongstoin (25°47'039.0"N 91°33120"E), which is located in West Khasi Hills District of Meghalaya, India at an average elevation of 1409 metres (4622 feet). West Khasi Hills District covers an area of 3911.22sq. km. and is bounded by Kamrup district of Assam on the north-west, Ri-bhoi district on the north-east, East Khasi Hills district on the east, by Bangladesh and South West Khasi Hills on the south, and East Garo Hills and South Garo Hills district on the west. Nongstoin is located 84km from Shillong, the capital city of Meghalaya. The area experiences a humid subtropical tropical, dry winter climate. The average rainfall ranges from 1200mm to 3000mm per annum (westkhasihills.gov.in).

The Lai Lyngdoh area in Nongstoin is a group of 34 villages which falls under the jurisdiction of the three Lyngdoh i.e. Marskuin, Nonglwai and Nongkhlaw located in West Khasi Hills District, Meghalaya. Marskuin is the only one Raid in the area. All of the villages are connected by road. Three local dialects are spoken here i.e., Nonglwai, Maram, and Marskuin.

In the present study, villages of Mawthungkper, Mynni mawbri, Nonglwai1, Nonglwai2, Nongklungrim, Nongklung, Marang, Nongkynjang, Byrki Mawthun and Pyndensohphoh were surveyed and interview were conducted with the locals, women folk, elderly and headmen of different villages were conducted in order to acquire information on the natural resources of the area. Documentation and photographs on agriculture produce, wild edibles, local tradition, etc. were recorded.

The information collection and documentation about ITK is done by interviewing local knowledgeable people including village elders, NGOs and fishermen and on the spot observation.

3. RESULTS AND DISCUSSION

The locals in the area mostly depend on the surrounding environment for their livelihood. From the surrounding forests and forest streams, a variety of minor products are harvested and a number of edibles which include wild fruits, leafy green, wild vegetables, mushroom, fish, frog, crustaceans, tubers and medicinal plants are also gathered. The main occupation of the people in Lai Lyngdoh includes shifting cultivation, agroforestry, basket making, vegetable cultivation, rice cultivation, poultry farming, pig farm, cattle farming, fisheries, and flower gardening.

Agricultural practice and agricultural products: The people in Lai Lyngdoh solely depend on agriculture and agricultural products. Agriculture is, therefore, the backbone for the livelihood of the people. The main agricultural practice in this area is rice cultivation. The other agricultural practices include jhum cultivation or shifting cultivation, vegetable cultivation

and agroforestry. The principal crops grown in the area includes potatoes, bay leaf, pepper, tapioca, sweet potatoes, citrus fruits, pineapples, bananas, etc.

Ka bri (Forest Garden) - Ka bri is the general term to any cultivated land in the Khasi Hills. Bri soh (fruit gardens) are mostly found in the area, but **bri kwai** (betel nut) and bri tympew (betel leaf) plantations are not practiced here. Cultivation of cash crop like broom grass, orange, pineapple, bay leaf, black pepper, food grains, colocacia, cucumber, potatoes, jackfruits are done on the hill slopes area.

Rep shyrtie (Shifting cultivation): Shifting cultivation is commonly practice in this area. It involves slash and burn farming. Some of the crops that are cultivated in shifting cultivation patches are *Solanum tuberosum*, *Manihot esculenta, Fagopyrum esculentum, Zea mays, Colocasia esculenta, Cucurbita moschata, Phaseous vulgaris, Zingiber offinale, Ipomoea batatas,* vegetables etc. Crops are planted and harvested only in one cycle i.e. only during the first year, and the area is replaced by broom or bamboo cultivation. An indigenous white tuberous delicacy known as Sohphlang (*Flemingia vestita*) is a common crop cultivated in the area grown from the months of September to February, where it is also planted in jhum areas. The root is edible and is a commonly consumed by the Khasi community. The local farmers sell this product in the nearby markets and in the town of Shillong.

Figure 1: *Fleminga vestita* (sohphlang)

Kper (Home Garden): A home garden is a farming system which combines different physical, social, and economic functions on the area of land around the family home. Kper produces a variety of food and other resources for both household consumption and for income generation. The main vegetables grown in home gardens (Table 1) are coriander, potatoes, pumpkin, basil, mushroom, pepper, lemon, broccoli, mustard, peas, green beans, brussel sprouts, tomatoes, bell peppers, beets, carrots, etc. Home gardens also produce crops like maize, which is commonly grown in the area. Flowers, orchids, tea and coffee are also grown in the area.

Chayote/Squash (*Sechium edule*), locally known as *Biskot*, is an edible plant belonging to the gourd family, Cucurbitaceae. It is a very prominent and abundant species, and is grown in the months of February-November in the villages of Mawthungkper, Mynni mawbri, Nonglwai1, Nonglwai2, Nongklungrim, Nongklung, and Marang. The locals build traditional support frames made of bamboo for the chayote to grow and extend, and these bamboo frames are usually replaced after a year or two.

Table 1: Vegetables grown in the home gardens in Lai Lyngdoh

Sl. No.	Botanical name	Family name	Common name	Local name
1	*Albelmochus esculentus*	Malvaceae	Okra	Bindi
2	*Allium fistulosum*	Amaryllidaceae	Welsh onion	Jyllang
3	*Allium cepa*	Amaryllidaceae	Onion	Piat
4	*Allium sativum*	Amaryllidaceae	Garlic	Rynsun
5	*Beta vulgaris*	Chenopodiaceae	Beetroot	Bit
6	*Brassica oleraceae var. botrytis*	Brassicaceae	Cauliflower	Phul kubi
7	*Brassica oleraceae var. capitata*	Brassicaceae	Cabbage	Kubi
8	*Capsicum annuum*	Solanaceae	Red capsicum	Sohsat jhur
9	*Capsicum frutescens*	Solanaceae	Chilli	Sohsat
10	*Coriandum sativum*	Apiaceae	Coriander	Dhunia
11	*Colocasia esculenta*	Solanaceae	Yam	Chriew
12	*Cucumis sativus*	Cucurbitaceae	Cucumber	Soh khwe
13	*Cucurbita moschata*	Cucurbitaceae	Pumpkin	Soh pyrlaw
14	*Daucus carota*	Apiaceae	Carrot	Kajor
15	*Ipomoea batatas*	convolvulaceae	Sweet potato	Phan karo
16	*Momordica charantis*	Cucurbitaceae	Bitter gourd	Kerela
17	*Phaseous vulgaris*	Fabaceae	Green beans	Prisbin
18	*Pisum sativum*	Fabaceae	Pea	Mator
19	*Raphanus raphanistrum sativus*	Brassicaceae	Radish	Sohlakum
20	*Sechium edule*	Cucurbitaceae	Chayote	Biskot
21	*Solanum melongena*	Solanaceae	Aubergine	Baingon
22	*Solanum lypopersicum*	Solanaceae	Tomato	Sohsaw
23	*Solanum tuberosum*	Solanaceae	Potato	Soh phan
24	*Solanum tuberosum*	Nightshade	King Edward potato	Phan saw
25	*Zingiber offinale*	Zingiberaceae	Ginger	Syieng

Bsah: This is one of the most environmentally method of cultivation and it is similar to agroforestry. In this type of cultivation, cash crops namely betel leaf, black pepper, are mainly grown with proper management of the natural forest because these crops require trees for their support and growth. Citrus fruits are also grown and other wild fruit are raised and managed (Table 2).

Table 2: Fruits cultivated in the villages of Lai Lyngdoh

Sl. No.	Botanical name	Family	Common name	Local name
1	*Actinia deliciosa*	Actinidiaceae	Kiwi	Soh kiwi
2	*Citrus limon*	Rutaceae	Lemon	Sohjew
3	*Citrus recticulata*	Rutaceae	Khasi mandarin	Sohniamtra
4	*Psidium gujava*	Myrtaceae	Guava	Soh pyriam
5	*Prunus persica*	Rosaceae	Peaches	Soh phareng
6	*Pyrus communis*	Rosaceae	Pear	Soh phoh
7	*Prunus domestica*	Rosaceae	Plum	Soh plom
8	*Prunus nepalensis*	Rosaceae	Sohiong	Soh iong
9	*Vitus vinifera*	Vitaceae	Grapes	Soh kraip

Bri soh (Fruit Garden): In Bri soh, citrus fruits such as *Citrus recticulata* (Khasi mandarin) is the main produce cultivated. Varieties of other vegetable crops are also grown in the same land.

Agroforestry – The people in West Khasi Hills practice agroforestry. This is an old indigenous method of cultivation where the economically important plants are grown and managed mainly in the form of a forest garden. A forest garden is an agroforestry system which mimics a natural forest which is sustainable, stable and low-maintenance and is created for the cultivation of food crops. Different types of plants are grown in these forests which include banana, oranges, black pepper etc. These forests are the main source of cash income for the local people. Agroforestry is practiced in some of the villages of Mawthungkper, Nonglwai1, Nonglwai2, Nongkynjang, Byrki mawthung, and Pyndensohphoh. Organic farming is practised for increasing the crop production and enhancing soil fertility. Moreover, marigolds are planted by farmers to eliminate agricultural pests.

Wild fruits and vegetables: The Lai Lyngdoh area is very rich in wild fruits and vegetables due to the availability of dense forests and favourable environment conditions. Wild fruits are collected and consumed by the locals (Table 3); wild animals in the forests also eat such fruits. Many fruits and vegetable (Table 4) are collected from the surrounding environment in the villages during different season of the year.

Table 3: Wild fruit in the forests of Lai Lyngdoh

Sl. No.	Botanical name	Family	Common name	Local name	Harvest period
1	*Eleagenus latifolia*	Eleagnaceae	Spiny oleaster	Sohchang	March-May
2	*Morus nigra*	Moraceae	Black mulberry	Soh sim	March-June
3	*Myrica esculenta*	Myricaceae	Box myrtle	Soh phei	March-June
4	*Myrica nagi*	Myricaceae	Box myrtle	Soh phei nam	March-April
5	*Prunus nepalensis*	Rosaceae	Sohiong	Sohiong	March-April
6	*Rubus ulmifolius*	Rosaceae	Black berry	Soh khariong	March-June
7	*Rubus ellipticus*	Rosaceae	Cheeseberry	Sohweit	March-June
8	*Viburnum foetidum*	Viburnaceae	Stinking viburnum	Sohlang	July-September

Table 4: **Wild vegetables in the forests of Lai Lyngdoh**

Sl. No.	Botanical name	family	Common name	Local name
1	*Allium tuberosum*	Amaryllidaceae	Garlic chives	Jwe lang
2	*Aristolochia pistolochia*	Aristolochiaceae	Pistolochia	Jathang
3	*Fagopyrum esculentum*	Polygonaceae	Silverhull	Jarain
4	*Houttuynia cordata*	Saururaceae	Heart leaf	Jwepyrtoh
5	*Mentha spicata*	Lamiaceae	Mint	Pudina

Mushrooms: Numerous edible mushrooms (locally known as *tit*) are found in the Lai Lyngdoh area (Table 5). The local people collect these from forests for food or to be sold in the markets. Nowadays, the people of Lai Lyngdoh area have also started the practice of cultivation of mushroom. Tit tung (*Lentinula edodes*) is one of the most prominent mushrooms of the area and has high commercial value. Mushrooms are collected during the month of April-May when the area receives the first rainfall of the year.

Table 5: **Edible mushroom from the forest of Lai Lyngdoh**

Sl. No.	Scientific name	Family	Local name	Harvest period
1	*Agaricus campestris*	Agaricaceae	Tit eitmasi	April-May
2	*Amanita caesarea*	Amanitaceae	Tit thlong	April-June
3	*Daldinia concentrica*	Hypoxylaceae	Tit siaw	May-July
4	*Gomphus floccosus*	Gomphaceae	Tit sin	May-June
5	*Lentinula edodes*	Omphalotaceae	Tit tung	April-May
6	*Pleurotus ostreatus*	Pleurotaceae	Tit tlai	May
7	*Ramaria* sp.	Gomphaceae	Tit syiar	July-November
8	Unknown		Tit lakhar	June-August
9	Unknown		Tit lap	June-July
10	Unknown		Tit tynrai	May-June

Paddy cultivation: Paddy cultivation, locally known as thung kba, is one of the main sources of income in the Lai Lyngdoh area. The cultivation is carried out in the months of May to November. *Khaw saw* or Red rice is also common in the area.

Bamboo cultivation: Villages in the Lai Lyngdoh area grow bamboo where nearly every house has their own bamboo patch in their property. Bamboos are utilized for various purposes such as making fence, huts, basket making, ladders, bridges, etc. Bamboo species present in the area are locally as *skhen, ktang* and *skhen langka.*

Orchids: The Lai Lyngdoh area is very rich in orchids which are mostly found in the forest areas growing in the wild (Table 6). They are found growing on the surface of rocks and on branches of trees. The forests of Nonglwai area have the most species of orchids, many of which are still not identified. A local, Bah Char, collects these unknown species and preserve them in a restricted area of the village. Villagers collect orchids for decoration or they are sold in the local markets for additional income. *Dendrobium* species are abundantly found in the area of Lai Lyngdoh.

Table 6: Diversity of Orchids found in Lai Lyngdoh

Sl. No.	Botanical name	Month of blooming
1	*Acampe rigida*	September
2	*Aerides multiflora*	June
3	*Anoectochilus* sp.	November
4	*Anthogomium gracile*	August
5	*Arundina graminiflora*	July
6	*Ascocentrum ampullaceum*	March

7	*Bulnophyllum odoratissum*	July
8	*Bulbophyllum griffihti*	September
9	*Bulbophyllum affine*	June
10	*Bulbophullum* sp.	December
11	*Calanthe* sp.	May
12	*Cleisocebtron pallens*	August
13	*Cleisostoma racemiferum*	August
14	*Crepidium accuminatum*	April
15	*Cymbidium* sp.	November
16	*Dendrobium fimbriatum*	May
17	*Dendrobium moschantum*	July
18	*Dendrobium chrysanthum*	July
19	*Dendrobium eriiflorum*	October
20	*Dendrobium hetrerocarpum*	March
21	*Dendrobium transparens*	June
22	*Dendrobium* sp.	May
23	*Eria stricta*	December
24	*Eria bipunctata*	August
25	*Eria bambusifloria*	November
26	*Eriodes barbata*	October
27	*Flickingeria* sp.	July
28	*Luisia* sp.	September
29	*Neogyna garderiana*	November
31	*Papilionanthe vandarum*	March
31	*Pleione malculata*	October
32	*Pleione praecox*	November
33	*Paphiopedilum hybride*	November
34	*Thunia alba*	July

Medicinal plants

A number of medicinal plants used in local herbal remedies are found in the villages and forests of Lai Lyngdoh. A few of the medicinal plants are enumerated below (Table 7) with a brief description of their uses.

Table 7: **A few of the Medicinal plants utilised in the villages of Lai Lyngdoh**

Sl. No.	Botanical name	Family	Common name	Local name	Uses
1	*Angelica sylvestris*	Apiaceae	Wild angelica	Dieng iaplap	Use for treating wound
2	*Ageratina adenophera*	Compositae	Crofton weed	Dieng soh pang khlieh	Paste is applied in wounds

3	*Aspilia mossambicensis*	Asteraceae	Wild sunflower	Jwetur	Use for stomach ache
4	*Agrimonia eupatoria*	Rosaceae	Agrimony	Phanrain	Use for treating skin diseases
5	*Centella asiata*	Apiaceae	Marsh pennywort	Sohkhliang syiar	Use as stomach ache
6	*Crassocephalum crepidiodes*	Asteraceae	Fireweed	Kynbad chynreh	Use for treating wound
7	*Lantana camara*	Verbenaceae	Common lantana	Tiew awieng	Use for treating skin burn
8	*Ludwigia palustris*	Onograceae	Hampshire-purslane	Jwesat	Use for treating chicken diseases
9	*Melastoma malabathricum*	Melatomataceae	Indian rhododendron	Tiewthlong	The root are use for those who have low nutrition
10	*Paris polyphylla*	Melanthiaceae	Love apple	Soh bsein	Use for treating wound and low Bp level
11	*Solanum nigrum*	Solanaceae	Common night shade	Sohsat rain	Use for treating low Bp
12	*Stellaria holostea*	Carophyllaceae	Greater stitchwort	Studsyiar	Use for treating skin diseases

Freshwater Aquatic resources

The streams and rivers in the villages are rich in aquatic resources. During the present study, a few of the species of catfish, sucker fish, carps including prawns, crabs and aquatic insects were caught and are listed below (Table 8).

Table 8: Freshwater Aquatic resources collected from streams and rivers in the villages of Lai Lyngdoh

Sl. No.	Scientific name	Family	Common name	Local name
1	*Acheilognathus* sp.	Cyprinidae		Byrthih
2	*Channa sp.*	Channidae	Catfish	Dohthli
3	*Glyptothorax* sp.	Sisoridae	Catfish	Dohplin
4	*Labeo rohita*	Cyprinidae	Carp	Dohkha bah
5	*Macrobrachium* sp.	Palaemonidae	Prawn	Skweit
6	*Geothelphusa dehaani*	Gecarcinudae	Crab	Thwom
7	*Parathelphusa* sp.	Gecarcinucidae	Crab	Thwom ktih
8	*Neocurtilla hexadactyla*	Gryllotalpidae	Northern mole cricket	Pait langbor

ITK used in connection with fish and fisheries:

The locals for catching fish and other aquatic resources from the water employ a number of fishing gears. Local made bamboo fish traps, fishing rods, bamboo spears and small fishing nets are employed for the purpose. The flowering plant chickweed, *Stellaria holostea* (Family – Caryophyllaceae), is locally used as a fish poison in ponds or small streams. The roots of the plant are mashed into a paste and introduced into water bodies. After about 20-30 minutes, the effect of the root poison is seen and fishes affected by the plant float to the surface and are easily collected.

The plant is for fish bait is Sohsying and Sohlang. Sohsying is also known as Jhalu and Sohlang is generally known as Dieng sohlang. It is used as fish bait. The fruit is used as bait for attracting and catching Mahseer and Hill trout (*Barilius* sp.)

4. DISCUSSION

Bioresources are seen to play an important role in the lives of indigenous communities in Lai Lyngdoh area and are not likely to lessen in eventual future. These resources, however, need to be valued and used sustainably so that they can continue to support the community. Traditional methods and ways in the use of bioresources is practised

and still preserved in the indigenous communities and the documentation of local culture and knowledge will play an important role in conservation process. Forests and their products provide numerous benefits for humans and for their survival. Judicious and sustainable use of bio-resources including forest resources should be approached to provide long-term sustenance to the locals who make their living by harvesting these resources. Important species in forests that have commercial value as food, animal feed, medicines, etc. should identified, quantified and encouraged to increase in their numbers so that they can be a means of supply of non-timber forest products for the local people. Shifting cultivation, though a primitive practice, still remains a source of lively hood among majority of the farmer of the Lai Lyngdoh area. Nowadays, a number of local customs and practices have disappeared and an abundance of the indigenous knowledge is at peril due to rapid changes in our modern world. It is therefore imperative to apply techniques to manage forests for the services and supply it can render, in a sustainable manner.

Presently, there is a growing interest in the role that ITK systems play in development. The finding of ITKs stretches the relevance of ITK as a resource that provides a basis for sustainable and environmentally sound approaches to fisheries and natural resource management

ACKNOWLEDGEMENT

The authors would like to thank St. Edmund's College, Shillong for all the necessary facilities. We also would like to express our sincere gratitude to the villagers and the Dorbar Shnongs for their cooperation and encouragement.

REFERENCES

[1] Fitzpatrick, D. (2005). Best Practice: Options for the legal recognition of customary tenure. *Development and Change 36(3)*, 449-475.

[2] Konstantinus, A., Rozakis, S., Maria, E-A. & Kesheng, S. (2018). A definition of bioeconomy through the Bibliometric Networks of the Scientific Literature. *AgBioForum 21(2)*: 64-85.

[3] Nongbri, T. (2003). Development, ethnicity and gender. Rawat Publication, New Delhi.

[4] Tynsong, H., Dkhar, M. & Tiwari, B.K. (2012). Traditional knowledge based management and utilization of bio-resources by War Khasi tribe of Meghalaya, North-east India. *Indian Journal of Innovations Development 1(3),* 162-174.

[5] Tynsong, H., Tiwari, B.K. & Goswami, R.K. (2009). Canopy birds as wild resource–an indigenous knowledge approach to sustainable hunting. *5th International Canopy Conference 2009: Forest Canopies, Climate Change and Sustainable Use*, 125-130.

[6] World Bank. (1997). Knowledge and Skills for the Information Age, The First Meeting of the Mediterranean Development Forum. Mediterranean Development Forum, URL: http://www.worldbank.org/html/fpd/technet/mdf/objectiv.htm

Spectrum: Science and Technology
A peer reviewed research Journal

The Journal

Spectrum: Science and Technology is a peer reviewed open access research journal published annually by the Research and Consultancy Cell of St. Anthony's College, Shillong, Meghalaya, India.

The primary goal of the journal is to publish double-blind peer reviewed research articles from the field of Science and Technology. The journal also aims at to give a platform for publication of original research articles by researchers across different fields of science. The journal looks for articles that can share new, modified or systematically arranged knowledge to promote substantive dialogue among the research scholars of the world. The journal accepts paper(s) with well-developed theoretical perspective, literature review, methodology/research design, and analyses/results.

The journal follows the style and referencing as per the guidelines prescribed in the website of the college at www.anthonys.ac.in. The manuscripts should be prepared strictly as per the specifications and the journal article template provided in the website. The journal accepts articles only in soft copy that should be sent at spectrum.st@anthonys.ac.in.

All correspondence related to the paper or journal may be addressed to:

The Chief Editor
Spectrum: Science and Technology
St. Anthony's College
Shillong- 793001
Meghalaya, India
Email: spectrum.st@anthonys.ac.in

SPECTRUM:
SCIENCE AND TECHNOLOGY

A Peer Reviewed Research Journal

St. Anthony's College, established in 1934, became the first institute of higher education of the Don Bosco Society worldwide. The college was accredited by NAAC from the year the year 2000 onwards. It was also awarded the status of College with Potential for Excellence (CPE) by UGC in 2006 and same was renewed in 2011. St. Anthony's College, Shillong is now stands as one of the best colleges of the country.

For office details :

at
www.anthonys.ac.in